SALS: Smart Adaptive Load Shedding: Final Report

May 4, 2019

INNOPOWER
INNOVATIVE POWER AUTOMATION

AALBORG UNIVERSITET

nord energi

FORSK EL
Energinet.dk

Table of Contents

1 Executive Summary

The establishment of a reliable grid with security of supply and high penetration of renewable energy requires a revision and improvement of the protection system, due to the major differences to conventional energy sources (e.g. the lower reliability and inertia of renewable energy sources already requires the installation of synchronous condensers in Denmark).

The introduction of CML (Customer Minutes Lost) and CI (Customer Interruptions) targets in recent years has led Transmission System Operators (TSOs) and Distribution System Operators (DSOs) to investigate ways of improving these two different performance indicators. Two of the major challenges are the prediction of the power flow direction and the usage of inflexible setting of protection devices, which can be overcome by developing predictive and adaptive capabilities, able to provide condition/state monitoring features in protection devices, rather than constant and predefined parameters incapable of adapting to the event scale and location settings. To maintain the security of supply that the customers are used to have and expect, the DSOs will unquestionably need to update their protection devices with modern smart protection schemes. This will involve considerable time, organization and investment, but it is essential if the society is serious about having a high penetration of renewable energy and a disconnection of the large fossil-based power plants.

One area of protection that can be improved is load-shedding, which consists in the disconnection of load when there is not enough generation in the grid. In this project, an intelligent load-shedding relay with decentralized control strategy was designed and tested. This new relay is able to minimise the load shed during emergency operation, reducing the impact to the consumers as well as the economic impact for the TSO/DSO and society. The algorithm developed for load-shedding was tested in laboratory under different situations of power system emergency control resulting in a matured version prepared for field test in the final stage of the project. The development of the relay consisted of three Working Packages (WPs) with different tasks and milestones.

WP 1 with the title of **"Research & Development"** was fully accomplished except the part of sensitivity analysis and reliability improvement, which was transferred and done in WP2. Instead of evaluating the idea in theory using ideal simulation scenarios, it was decided to perform the analysis in WP2 under more realistic situation on the physical product of project. Therefore, the reliability of the algorithm was tested on the latest version of the algorithm using HIL before the field test.

"Controller Implementation in RTDS" was the title of **WP 2** with the aim of implementing the algorithm (relay controller) in a Real Time Digital Simulator (RTDS). The modelling of power system and controller in RTDS, the programming of the prototype relay and testing, plus debugging of algorithm were the main objectives of this working package. This working package was successfully finished.

WP 3 entitled **"Controller as Hardware in Loop (HIL)"** consisted in connecting the physical relay controller to the virtual power system simulated in RTDS as first task and to a physical relay is a substation as second task. The second task of WP3 is was two months delayed due to one team member changing job. The HIL test was made in a more realistic power system case study (39 bus system) followed by addressing the sensitivity analysis and reliability improvement of controller algorithm as HIL. Afterwards, the controller was installed at Agersted Substation operated by Nord Energi. The results show that the proposed algorithm behaves as expected.

In summary, the projected developed, implemented and demonstrated an algorithm able

to reduce the load shed amount, with the following features:

- Automatic tuning of protection relay settings.
- Decentralized and self-healing scheme.
- Reduce the number of load feeders involved in the load-shedding scheme.
- Over-frequency avoidance by preventing overload shedding.
- Localised load-shedding.
- Event location-oriented performance of smart relays.

2 Introduction

2.1 Project Objectives and Outcomes

Load Shedding (LS) is the last firewall and the most expensive control action against power system blackout. In the conventional Under Frequency LS (UFLS) schemes, the load drop locations are already determined independently of the event location. Furthermore, the frequency thresholds of LS relays are prespecified and constant values which may not be a comprehensive solution for the widespread range of possible events. This project addresses the decentralized LS in which the instantaneous voltage deviation of load buses is used to determine the frequency thresholds of LS relays. The higher frequency thresholds are assigned to the loads with larger voltage decay which are often located in the vicinity of disturbance location. The frequency thresholds of different relays are continuously updated based on the location and magnitude of the disturbance/s. The proposed method simultaneously benefits from individual UFLS and Under Voltage LS (UVLS) features which operate in the power system without coordination.

The method proposed in this project can easily handle the structural changes of the network, consequence of the uncertain connectivity of renewable energy sources, and paves the way toward Plug-and-Play (PnP) operation enabling the addition and removal of the system elements in a modular fashion way, by means of an automatic and adaptive up-dating the hardware setting according to the current state trajectory of the power system. This approach has the advantage on requiring minimal human intervention and it is especially advantageous in the large power systems, with time-varying connectivity of dispersed generations and in which big data is required to be processed in the control center. Moreover, the proposed method minimizes the consequences of communication lost, as well as addresses the increasing concerns with Cyber Security.

Main Objectives:

1. To reduce the load shed amount during emergency control;
2. To reduce the number of load feeders involved in the load shedding scheme;
3. Over frequency avoidance by preventing over load shedding;
4. Localized of load shedding;
5. Automatic tuning of protection relay settings;
6. Adaptive, decentralized and self-healing scheme;
7. Event location-oriented performance of smart relay.

2.2 Load Shedding

For a smooth growth of load, unit governors measure the speed decline and increase power input to the generator. Therefore, overload is compensated by using available spinning reserve, i.e. the unused capacity of all generators operating and synchronized to the system. If all generators are operating at maximum production capacity and hence there is no available spinning reserve, the governors may be unable to relieve extra loads. In any case, the fast frequency plunges that accompany serious overloads require impossibly rapid governor and

boiler reaction. To prevent such a drop in frequency, it is compulsory to intentionally and automatically release a portion of the load equal to or greater than the extra load. While the decline has been arrested and the frequency returned back to its normal range, the disconnected load may be retrieved in small amounts, in order to allow the spinning reserve to become active and any additional available generators to have enough time to start up and being available.

The frequency information in an integrated system is same for all different voltage levels and all consumers are equally affected by a frequency event. Load curtailment at any voltage level will improve the status of the whole network. To stop the frequency decline and subsequently to rise the frequency back into the normal range, more load should be shed than corresponding shortage. It is worthy to shed as little as possible amount of load above absolute necessary quantity. Actually if so much load is curtailed, the system may be lead to an unstable condition. Thus a measure of proper control should be included.

When a load shedding procedure is designed for a given power system, several key factors must be determined to achieve the most effective and optimal solution. There are several key parameters that should be carefully determined to minimize the amount of load to be curtailed, due to their significant effect on load shedding process. The total amount of shed load, the number of load shedding stages, the amount of stage shed load, frequency thresholds, the delay between stages and the location of load curtailment are important decision parameters which affect the load shedding process [1, 2].

In the decentralized strategy of load shedding, in which there is no communication link available for the distributed stability protection relays, locally measured voltage can be utilized to manage load shedding process according to the power system dynamics, especially making the scheme adaptive to the event location. The key role/impact of voltage dynamics in reflecting the power system stability status is discussed in details in the next section.

2.3 The Role of Voltage Dynamics in Power System Stability

A voltage collapse in a part of a power system indicates that the existing generators and transmission lines can not supply part of the load, which has gone beyond its normal operating range. More importantly, if this problem is not resolved in time by taking proper control actions, there is a risk of propagation of that local problem to a wider area or even to the entire network. Exploration of major blackouts, which happened in the late 1990s and early 2000s (the 1996 Western North America, the 2003-2004 Outages in Europe, 2003 eastern North America and others) demonstrated that the root cause of many of these blackouts was voltage collapse rather than the prevalent frequency event [3, 4]. It can be seen that voltage collapse can be a leading symptom of impending power system contingencies. There are new design and security issues that should be considered in an Under Voltage Load Shedding (UVLS) scheme and merely relying on Under Frequency Load Shedding (UFLS) schemes and issuing a relevant control action can not be a remedial countermeasure for a wide range of disturbances especially disturbances with under voltage initiating events, since they may not be an appropriate countermeasure for voltage collapse situations.

Nowadays, the growing concern about the incidents initiated by voltage root causes has located it in the center of attention [5]. Besides, assigning a separate category of instability classification to the voltage instability shows the importance of voltage dynamical behavior in the power system stability area [6]. The significance of voltage profile was stressed from different aspect of views in many literatures which are briefly reviewed in this section [7, 8].

The shortage of active power is often accompanied by deficit in reactive power and the lack of active/reactive power is reflected in the voltage profile of the load buses [9]. Any LS scheme in which the dependency of the loads to the voltage variation is overlooked may not be effective in practice.

According to [6], the voltage instability is a phenomena of a local nature and if it is not prevented in time by proper control actions, it may spread to neighbor areas and even to the entire power system. Since the frequency which is measured locally at load buses is a common factor across the whole network and does not contain useful information about the event location, the voltage instability and its geographical region may be detected only based on the voltage data.

In the decentralized control strategy which is the main effort of the present work, there is no communication link between relays involved with LS scheme. Therefore, the magnitude and location of the event are unavailable. Although, the aforementioned information are unknown and unaccessible in a decentralized LS scheme, the voltage deviation is linearly determined by them [10]. Hence, a more accurate and reliable measure of sensitivity to the scale and place of perturbation is the voltage deviation of load buses, i.e. a quantity that is locally available. The sensitivity of each individual load bus to a given incident may be reflected via their voltage deviation. It means that the load buses with more sensitivity to the disturbance, experience a larger voltage drop. Therefore, the load buses may be classified in term of their voltage drop which is proportional to their sensitivity.

Utilizing the voltage drop data in the centralized strategy of the LS program have been proposed by numerous literatures as an appropriate and efficient criterion for determining the location of disturbance [9, 11–13], but application of voltage decay has rarely been employed in the decentralized strategy, especially for on-line and dynamically determining the frequency set points of the LS relays.

Conventional emergency control schemes that merely use the frequency data in LS plan and coordination of frequency and voltage are rarely considered in protection schemes in practice. For the sake of the aforementioned reasons, voltage information alongside frequency data is recently taken into account as a key factor that shows if the power system is under stress or not [1]. Power system operators recognize that frequency may remain in normal range during the voltage sags before the entire system collapse and are going to employ the UVLS scheme as a complementary part of their existing UFLS scheme.

2.4 Coordination of UVLS and UFLS Schemes

According to [14] regarding impacts of voltage variation on UFLS scheme, a precise perception of the characteristics of both frequency and voltage collapse is necessary to establish a proper and effective coordination between underfrequency and undervoltage tripping schemes. Underfrequency and undervoltage collapse are to some extend independent incidents and may typically have distinct root causes such as loss of a huge generation for underfrequency or outage of a determinant transmission line for undervoltage collapse. Undervoltage event is identified as a local phenomena, whereas underfrequency event is classified as a global system incident. Generally, voltage collapse influence the frequency profile slightly, which may not be sufficient enough to make the underfrequency schemes to react.

A remarkable generation lost may namely lead to a load-generation imbalance throughout the whole system following by an underfrequency incident. The frequency starts to drop gradually with the event, but typically not as fast as undervoltage events due to long inertia

time constants of system generators in conventional power systems.

Voltage incidents are generally associated with the local lack of reactive power. A slow voltage drop may come from reaching the generator to full capacity of available reactive power reserve and a fast voltage decline can be typically involved to serious disturbances such as transmission line short circuit or loss. Voltage collapse can come to exist in areas, which either the load is supplied by a faraway generation with restricted reactive power support or areas with a low level of local generation and a high portion of motor loads. Undervoltage events often happen in a shorter range of time in comparison to underfrequency events.

Undervoltage and underfrequency load shedding plans have different characteristics and are independently established in power system without any coordination. Study of UFLS scheme is often carried out using the System Frequency Response models (SFRs) [9, 11, 15]. The effects of voltage changes on the frequency deviation is not taken into account in these models. Contrariwise, the UVLS methods that have been proposed so far for setting of the UVLS relays, do not employ the frequency indices [2, 16]. Combination of both schemes seems to be necessary in practice to achieve a more reliable/effective LS scheme. Any individual use of these indices may lead the power system toward over load shedding or blackout. Decentralized UVLS scheme may be employed to avoid local voltage collapse at many substations. By sharing the existing software and hardware between both undervoltage and underfrequency protection schemes, the UVLS scheme can be implemented in parallel with underfrequency in order to be economically affordable.

2.5 LS Localization Using Voltage Drop Data

Determining the locations of LS is one of the most important key factors, which needs to be selected carefully. In order to obtain a more reliable/efficient LS plan during emergency conditions, the event location must be properly included in the decision making process, whereas in the conventional UFLS schemes, the loads, which should be dropped in case of need to LS are already determined independent of contingency location and current status of power system [11, 17]. Discarding the loads, which are distant from the event location, may cause overloading of tie-lines, power factor reduction and even worse voltage profiles [18]. Inversely, dropping the loads located inside the neighborhood of disturbance point may recover the voltage of affected load buses and is strongly recommended by many literatures [7, 12, 15].

The loads may be prioritized to discard based on their voltage decay, i.e. the loads with larger voltage decay are curtailed sooner than the others. The LS process begins to be triggered from the failure zone and radially proliferates in the network in such a way that not only the frequency downfall is stopped in time, but also the frequency comes back into the permissible range [7, 19]. Therefore, according to [9, 12], in order to find the most appropriate locations for the LS plan, the deviation of the load bus voltages may be a proper and effective criterion of proximity to the event location.

The voltage data involved in the proposed method are accessible even in the conventional LS relays. In the present decentralized UFVLS scheme, the expenses and vulnerability of communication system are avoided and by sharing the existing software and hardware available inside the LS relays between both UVLS and UFLS schemes, practical implementation of approach may financially be affordable [17, 20].

3 Power System Modeling

3.1 Power System Simulator Tools

3.1.1 Real Time Digital Simulator (RTDS)

Real Time Digital Simulator (RTDS) shown in Figure 1 is a powerful computer that performs the real-time simulation via parallel computation. The hardware accomplishes the time-domain simulations at real-time speed using time steps equal to 50 μs. Such a small time-steps is accurate enough for the RTDS to precisely simulate power system phenomena in the range of 0 to 3 kHz, which fully covers the dynamical behavior of conventional power systems.

The power system structure is constructed in a Graphical User Interface (GUI) software called RSCAD. This software dedicates a comprehensive library covering numerous power system components and control models. The RSCAD includes two major modules, Draft and Runtime. First, the power system is modeled and compiled in Draft. Then, the Draft transfers the resultant compiled file to the hardware, i.e. rock/s. The Runtime executes the simulation on rocks in real-time and provides simulation results for user. The user can influence the power system by interacting with the simulation in real-time via applying different changes to the components and their parameters, the topology, defining the events, etc. RSCAD can alternatively import the power system structure/data files from other commonly used formats e.g. PSS/E, in order to avoid remodeling of the system in Draft and being more user friendly.

3.1.2 PowerFactory (Digsilent)

DIgSILENT PowerFactory is a leading integrated power system analysis software, which covers the full range of functionality from standard features to highly sophisticated and advanced applications including wind power, distributed generation, real-time simulation and performance monitoring for system testing and supervision. For wind power applications, PowerFactory has become the industry's standard tool, due to comprehensive models and algorithms providing unrivalled accuracy and performance. DIgSILENT StationWare is a reliable central protection settings database and management system, based on the latest .NET technology. StationWare stores and records all settings in a central database, allows modeling of relevant work flow sequences. It provides quick access to relay manuals, interfaces with manufacturer-specific relay settings and integrates with PowerFactory software, allowing powerful and easy-to-use settings coordination studies.

3.2 Power System Elements

3.2.1 Synchronous Machines

The synchronous machine model is based on generalized machine theory. The model may be connected to an arbitrary power system defined by user in Draft module of RSCAD. As shown in Figure 2, control blocks of excitation and governor systems associate with the synchronous machine also need to be separately modeled. These control blocks are not included internally in the machine model, and therefore, standard Exciter and Governor/Turbine models available in the RSCAD library can be interfaced through the external connections provided on the synchronous generator.

The generalized machine model transforms the stator winding voltages into equivalent commutator winding voltages, using the dq0 transformation. The three phase rotor winding are also transformed into a two-phase equivalent winding, with additional windings added to each axis to fully represent that particular machine. The model uses fluxes as state variables

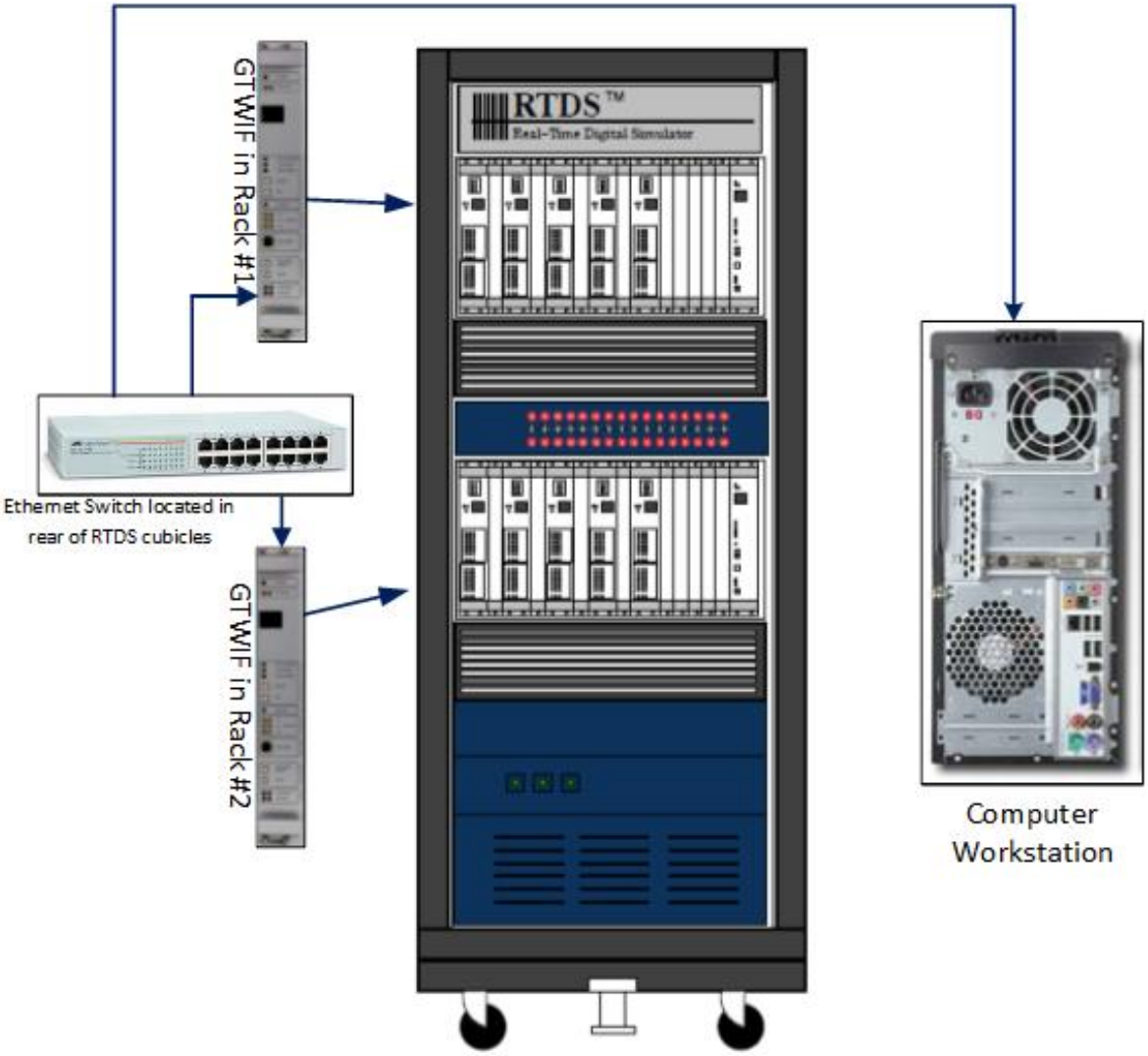

Figure 1: Typical configuration of RTDS

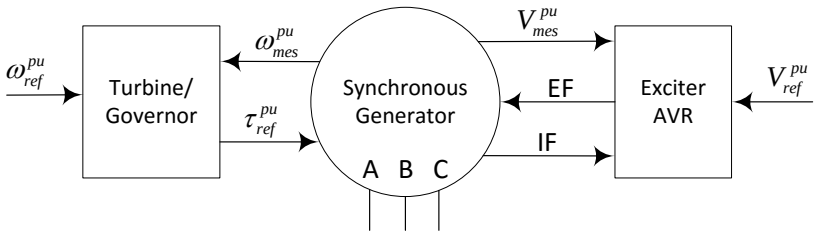

Figure 2: Synchronous machine control structure

rather than currents. Calculation of winding currents based on winding fluxes allows the resistance drop in the windings without need to a one step delay in the simulation. This technique enhances the accuracy of damping at high frequencies.

Equations representing a single rotating mass are solved within the synchronous machine model. However, in some cases it is necessary to study the interactions between various masses which are connected to a common shaft. Turbine models have been developed to accurately represent the dynamics of many masses connected to a single rotating shaft. The models are presently dimensioned to accommodate 6 masses, e.g. several turbines and 1 generator. The effects of multiple shaft masses are separately modeled using the Multi-mass Torsional Shaft component, which is directly interfaced with the machine model.

The startup of large power systems with numerous synchronous generators, especially if they include a multi?mass representation is normally accompanied by transient oscillations. In order to start from a steady state with a flat simulations, it is necessary to run a load?flow solution to determine the system power flows, which are desired. The load flow results are utilized as initial condition for generator and source models. Therefore, even if all machines have initial conditions set, there will still be an electrical startup disturbance due to the time required for the electrical system to reach the steady state.

The model contains a built-in and optional Y-Δ transformer, which accepts zero sequence parameters. By enabling the transformer the corresponding three nodes between the generator and the transformer are also included in the simulation and therefore, the number of nodes are increased comparing to the case of single lumped network simulation. Moreover, the model also procures optional resistive, inductive and capacitive load types connected to the machine terminals.

3.2.2 Active Voltage Regulator: Exciter (AVR)

Various IEEE Standard exciters are available for voltage regulation purpose. The distinct input/output variables of exciter indicated in Figure 2 are provided in per-unit (pu) and are briefly described as below:

- V_{mes}^{pu}: [Input] This input receives the measured RMS voltage of synchronous machine terminal.
- V_{ref}^{pu}: [Input] This input receives the voltage reference for the synchronous machine terminals.
- IF: [Input] This variable represents the field current of synchronous generator to be passed to the exciter. It may be applied within the exciter model for saturation and/or compensation.
- EF: [Input] This output is the computed field voltage applied directly to field winding of synchronous machine.

Figure 3 depicts different control strategy for either voltage (V) or reactive power (Q) regulation. The sub figure 3a illustrates how the voltage reference (V_{ref}^{pu}) of exciter can be determined based on the desired voltage set point (V_{set}^{pu}) using provided switch. Under this circumstances (V mode), sufficient reactive power is injected to the power system to regulate the voltage on the set point. Flipping the switch position, changes the control mode from V to Q, which means that regardless of the grid voltage variations, constant reactive power

(Q^{pu}_{ref}) is injected to the power system. To this aim, the difference between the measured reactive power and reference as error signal is fed to a PI controller to provide the voltage reference signal. Practical upper and lower limits are applied to the resultant signal to avoid out of range voltages.

Figure 3b represents calculation of reactive power reference (Q^{pu}_{ref}) using a desired set point (Q^{pu}_{set}). If operation of generator under a desired Power Factor (PF_{set}) is required, this capability may be selected using corresponding switch. Figure 3c specifies the upper and lower limits of reactive power range using the apparent power and measured active power of generator in pu. In this case, the reactive power support of grid is fulfilled using the spinning reserve available in the generator.

3.2.3 Active Gain Controller: Governor (GOV)

Simulation of mechanical transients traditionally falls within the realm of stability, where the modeling detail is not as complete as they are in an electromagnetic transient program.Generally, the electromagnetic transients are often faster (wider frequency band pass) comparing to the mechanical dynamics. Governors can be interfaced with a synchronous generator by either directly providing of input mechanical torque signal or through interaction with a corresponding turbine model (depending on the governor type). Both hydro and thermal (steam) governors of type standard (IEEE) governors are available in the Master Library.

The inputs of the governor/turbine model are the generator speed (ω^{pu}_{mes}) and the speed

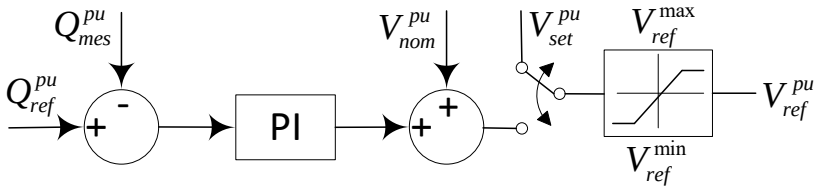

(a) Voltage reference based on voltage set point or reactive power reference

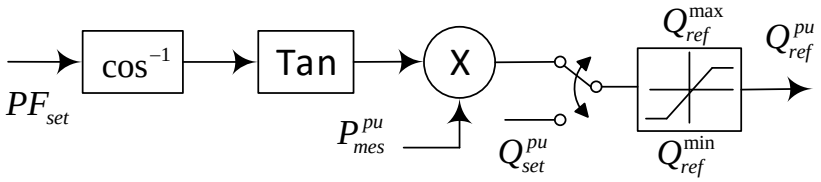

(b) Reactive power reference based on Power Factor (PF) or reactive power set point

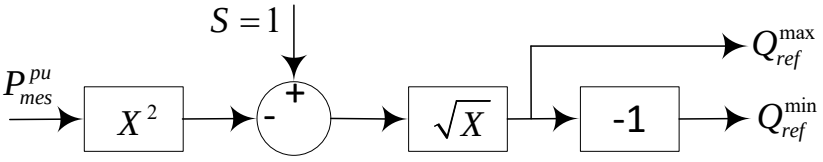

(c) The upper and lower limits of reactive power

Figure 3: The overall control strategy of voltage/reactive power regulation

reference (ω_{ref}^{pu}) in per-unit. The output is the mechanical torque (τ_{ref}^{pu}) from the HP and LP turbines (figure 2). There is the possibility to set the operation mode of generator on Frequency (F) control mode as a slack generator or constant Power (P) mode. Figure 4 shows both control modes of synchronous generator. In figure 4a the speed reference is determined using speed set point (ω_{set}^{pu}) or constant power production. The power error is calculated using the difference between the power reference (P_{ref}^{pu}) and the measured active power (P_{mes}^{pu}). The power error signal is passed through a PI controller to provide the speed reference (ω_{ref}^{pu}). Figure 4b indicates the same control strategy for Power or Frequency control modes. Selection of constant torque option provides production of constant power and adjusting the torque to achieve the speed reference (ω_{ref}^{pu}) yeilds the frequency control mode.

3.2.4 Loads

Considering the impact of voltage dynamics on the load?s behavior is strongly recommended by many literatures [9, 21]. In contrast, the influence of frequency variations on the load?s active and reactive power can be overlooked without sacrificing the accuracy of simulation results [9]. The voltage dependency of loads can be modeled as below:

$$P = P_0 \cdot \left(s_z \cdot (\frac{v}{v_0})^{pvz} + s_i \cdot (\frac{v}{v_0})^{pvi} + s_p \cdot (\frac{v}{v_0})^{pvp} \right) \tag{1}$$

$$Q = Q_0 \cdot \left(s_z \cdot (\frac{v}{v_0})^{qvz} + s_i \cdot (\frac{v}{v_0})^{qvi} + s_p \cdot (\frac{v}{v_0})^{qvp} \right) \tag{2}$$

where $s_p = 1 - s_z - s_i$. The subscript 0 stands for nominal values. The quantities P, Q and v represent active, reactive power and voltage, respectively. The composition of different types of load including constant impedance (s_z), current (s_i) and power (s_p) in a typical load feeder is presented in Tab. 1 [7]. The exponents mentioned in (1) and (2) have been summarized in different columns of lookup table, e.g. constant pvz specifies the exponent for dependency of active power to voltage for constant impedance load type.

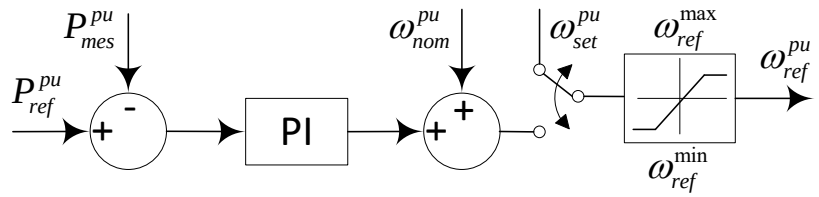

(a) Speed reference based on speed set point or active power reference

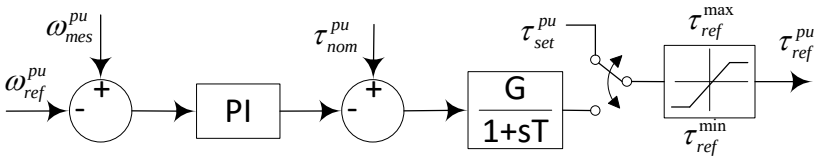

(b) Torque reference based on torque set point or speed reference

Figure 4: The overall control strategy of frequency/active power regulation

3.2.5 Load Shedding Relay

Fig. 5 indicates the cubical structure of bus B_i and distribution of load between existing substation feeders. Four feeders F_1^i to F_4^i in accordance with the typical and existing load shedding relays in the market with relevant circuit breakers are assumed to be available in the busbar. The corresponding four frequency setpoints/thresholds can be arbitrarily assigned to the relays/feeders, if prioritization is required in a particular busbar.

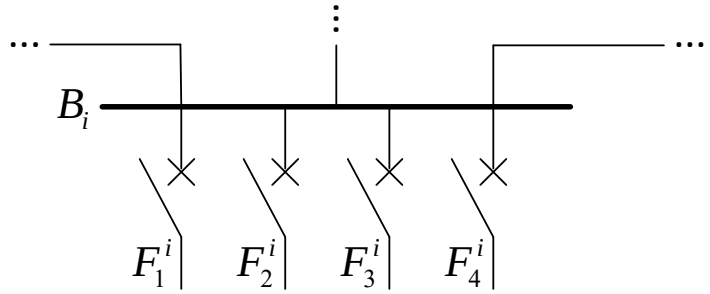

Figure 5: Typical configuration of load bus feeders

Table 1: The Voltage & Frequency Dependency of Loads

Load type	**Share** $(s)(\%)$	pv	pf	qv	qf
Light bulb (z)	10	1.6	0.0	0.0	0.1
Fluorescent bulb (i)	20	1.2	-1.0	3.0	-2.8
Asynchronous motor (p)	70	0.1	2.8	0.6	1.8

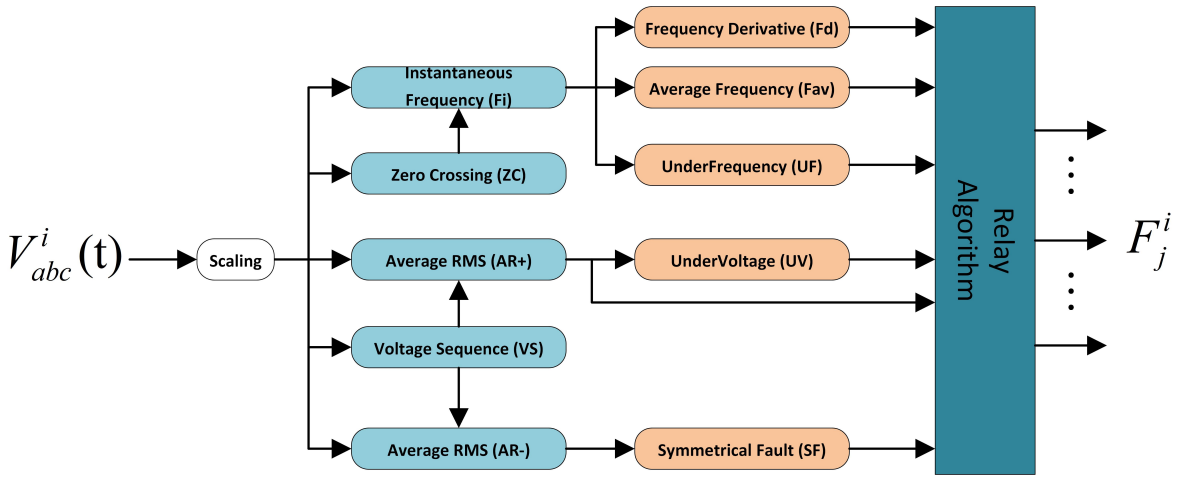

Figure 6: Block diagram of load shedding relay

4 Controller Algorithm

Fig. 6 illustrates distinct submodules, which provide different signals required to achieve desired performance of relay algorithm depicted at right side of block diagram. The three phase voltages (V^i_{abc}) of load bus i are downscaled to a proper level using available PT transformer.

The submodules are briefly listed below and are discussed in details in there corresponding sections:

- **Zero Crossing (ZC)**): This module detects Zero crossing of three phase voltages to calculate period of waveform.
- **Instantaneous Frequency (Fi)**): This module calculates the instantaneous frequency using the time gap between each consecutive zero crossing of three phases.
- **Average frequency (Fav)**): In this block, the average of frequency is calculated using a given number of the latest samples
- **UnderFrequency (UF)**): Here, the time in which the frequency crosses down the higher frequency threshold of load shedding scheme is detected to be considered as the base time.
- **Frequency Derivative (Fd)**): in this module, the frequency gradient is estimated and filtered.
- **Voltage RMS (VR)**): The rms value of three phase voltages is calculated after each cycling time.
- **Voltage Sequence (VS)**): In this submodule, the magnitude of positive, negative and zero sequence of three phase voltage are calculated.
- **UnderVoltage (UV)**): Here, the time in which the rms voltage crosses down the higher voltage threshold of load shedding scheme is detected.
- **Symmetrical Fault (SF)**): In this block, load shedding scheme is blocked if the negative sequence of voltage is observed higher than the threshold recommended by relevant standards.

The submodules associated with the frequency measurement, specified with where in Fig. 6, have been successfully tested on both virtual relay (the simulated relay in RTDS) and the physical relay connected to the RTDS via Hardware in Loop (HIL). The performance of submodules has been validated through ideal conditions.

The rest of submodules (unticked) are relevant to processing of voltage signal, which are required for detection and blocking of asymmetrical faults. Therefore, the absence of aforementioned blocks do not affect the normal operation of relay for three phase symmetrical faults. Implementation of voltage submodules are included in the reliability and sensitivity analysis.

4.1 Stage Frequency Thresholds

The frequency set points of the load shedding relays are automatically calculated based on voltage drop data at the corresponding substation bus. The loads with more voltage decline are relatively allocated higher frequency set points. The voltage drop ($\Delta v_i(t)$) at a given bus i can be determined using subtraction of its steady state quantity (v_i^{ss}) or 1 pu from its instantaneous value $v_i(t)$:

$$\Delta v_i(t) = v_i^{ss} - v_i(t) \tag{3}$$

There are two different possibilities to be considered as the pre-disturbance voltage magnitude. Each individual choice, has its positive and negative consequences. In order to make the scheme adaptive to the event location, the steady state value of voltage, i.e. v_i^{ss} should be considered for voltage drop calculation. In this case, having bus voltages close to their high limit (1.05 pu) located in the vicinity of event location may cause out of range voltages as a consequence, which is not desired.

Another alternative is selection of 1 pu, which concentrates the control action on the substations with relatively lower voltage profile, no matter how close or far they are to the faulty region.

The first frequency set point (stage 1) of relay i can be determined as below inside the range of f_h=59.3 Hz to f_l=58.4 Hz [22]:

$$f_i(t) = f_L(t) + (f_h - f_L(t)) \cdot \Delta v_i(t) \tag{4}$$

The IEEE and NERC standards associated with plant protection system of synchronous machines defines the maximum permissible time of being out of range for frequency following contingencies. The plant protection standard emphasizes that not only the out of range frequency, but also the frequency collapse time duration is also determinant in triggering the plant protection relays [7, 23–25]. In order to prevent activation of plant protection system following sever disturbances, the proposed approach can be coordinated with the criteria mentioned in NERC standard [22]. The lower limit of frequency range ($f_L(t)$) for load shedding thresholds can be determined as below in order to be sure that the frequency will not be allowed to be less than a certain value (e.g. f_h) for a duration more than a specific period of time (e.g. T_h):

$$f_L(t) = \begin{cases} f_L = 58.0 & t \le T_L = 2 \\ m \cdot \log(t) + b & T_L \le t \le T_h \\ f_h = 59.3 & t \ge T_h = 60 \end{cases} \tag{5}$$

where

$$m = \frac{f_h - f_L}{\log(T_h/T_L)} \quad , \quad b = f_h - m \cdot \log(T_h) \tag{6}$$

The LS scheme is triggered when the frequency declines below f_H, and therefore the corresponding time is selected as the origin of the time axis:

$$t = 0|_{f(t)=f_H \& \dot{f}_{av}(t)<0} \tag{7}$$

4.2 Adaptive Stage Time Delays

In the future power systems with high share of non synchronous generation type, the inertia of power system will be less, but more importantly unknown and uncertain. Even none-severe disturbance/s may lead to fast frequency drop, which make the situation even more

unpredictable. Therefore, the available reaction time for control actions will be less, when the frequency declines fast. In order to be able to harness the frequency drop, the time delay between successive stages needs to be adaptive to the Rate of Change of Frequency (ROCOF). The time dealy as a function of number of cycles can be defined as below:

$$N_i(t) = N_{\min} + (\frac{N_{\max} - N_{\min}}{\dot{f}_{\max} - \dot{f}_{\min}}) \cdot (\dot{f}_{av}(t) - \dot{f}_{\min}) \tag{8}$$

where N_{min} and N_{max} represent the minimum and maximum time delay in term of number of cycles to be respected between each two successive frequency set points regarding relay and circuit breaker operation time, in which under any circumstances, should not be less than 6 cycles [7, 22]. The number of cycles in the range of 10 - 14 is typically recommended by relevant IEEE standards [7].

$$10 \leq N_i(t) \leq 14 \tag{9}$$

The maximum and minimum possible quantities for ROCOF are introduced by $\dot{f}_{\max}$ and $\dot{f}_{\min}$, respectively. $\dot{f}_{\min}$ may be as low as -1 Hz/sec for severe contingencies and/or very low inertia power systems.

4.3 Under Voltage/Frequency Detection

In the power system stability and control, not only out of range variables should be considered in the decision making procedure, but also the time of being out of range is determinant. It means that we can not expect power system equipment to operate out of range for a long time beyond their protection system settings. Therefore, the time in which the key variables such as frequency and voltage cross their permissible range should be registered.

Since the frequency and voltage may experience transient oscillations due to local and/or interarea modes, it is required to consider a security margin for the time of being out of range. The time in which under frequency is detected can be defined as below:

$$T_{uf} = t \quad if \quad f_i(t) \leq f_h|_{m \cdot T_n} \tag{10}$$

where T_{uf} is the time of under frequency occurrence and T_n is the power system cycle time. The dead band for time delay is counted in term of number of cycles represented by m. The typical values for m can be found in the manual of ordinary relays in the market relay.

In a same manner, the under voltage phenomena can be recognized and its occurrence time can be registered as follows:

$$T_{uv} = t \quad if \quad v_i(t) \leq 0.95\ pu|_{m \cdot T_n} \tag{11}$$

4.4 Algorithm Flowchart

Fig. 7 summarizes the decision making procedure of the algorithm demonstrated in the controller. In the first diamond checkpoint of the flowchart, the frequency is monitored to be sure the controller will be triggered if the frequency declines to a value below f_t. The second checkpoint is about having negative ROCOF as a precondition for controller activation. Respecting sufficient time delay between consecutive stages are assured in the third diamond checkpoint. The last but lot least condition is associated with identification of fast enough frequency recovery trend before any plant protection relay can be triggered leading to outage of power plants.

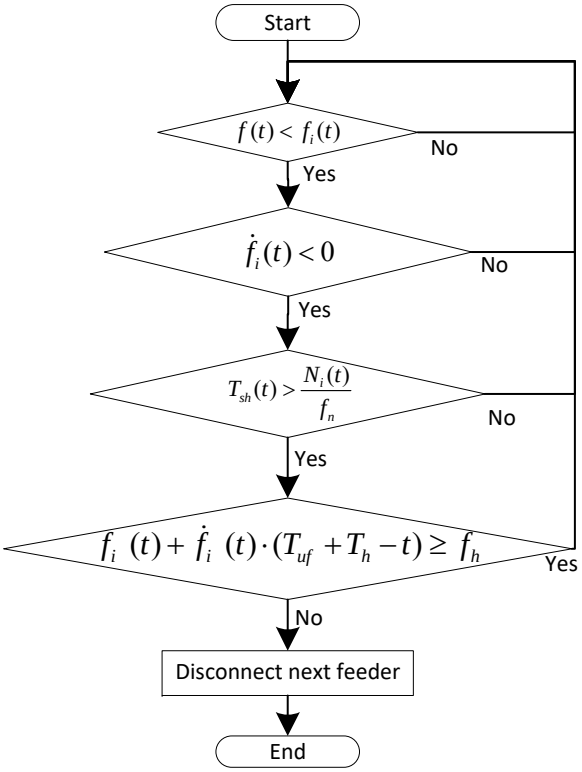

Figure 7: Feeder disconnection decision & proposed flowchart

4.5 Power System Case Studies

4.5.1 IEEE 9 Bus Standard Test System

In order to evaluate the superiority of proposed control scheme, the WSCC 3-machine system which is well-known as P.M Anderson 9-bus is chosen as the first case study. The power system contains of 3 generators, 6 lines, 3 two winding power transformers and 3 loads as depicted in Fig.8a. The static and dynamic data of the system can be found in [26]. Meanwhile, the synchronous generators are equipped with IEEE standard governor GOV-IEESGO and automatic voltage regulator AVR-IEEEX1.

4.5.2 IEEE 39 Bus Standard Test System

The 39 Bus test System is a relatively simplified model of the high voltage transmission system in the northeast part of the USA, i.e. New England area. It was presented for the first time in 1970 and has since been widely used for scientific research and publications. This section describes its structure and parameters.

The 39 Bus test System consists of 39 buses, 10 generators, 19 loads, 34 lines and 12 transformers (Fig. 8b). The nominal frequency of the network is 60 Hz and the mains voltage level is 345 kV. Generator G1 is the equivalent circuit representing the interconnection to the rest of the transmission system (U.S. and Canadian) and is therefore directly connected at the 345 kV level. All other generators are connected via transformers. Generator G2 is the slack generator of the network with voltage magnitude and angle equal to 0.982 p.u., 0.0

degrees, respectively.

5 Controller As Hardware in Loop (HIL) of RTDS

5.1 Controller and RTDS Hardware Interface

The hardware setup by means of equipment arrangement and interface is presented in figure. 9. Figure. 10 indicates the signal flow of power and control regarding the interface of controller and the power system simulated in RTDS. The prototype controller is connected to the RTDS according to the details of hardware interface illustrated in Figure. 10. The physical controller with the algorithm programmed in its memory is utilized as load shedding relay installed at load bus 5. The controller for the rest of load buses, e.g. load 6 and load 8 are still simulated inside the RTDS.

The Potential Transformer (PT), indicated in figure. 10, steps down the three phase sinusoidal waveform of bus voltage to the range of 220 volt (rms) inside the RTDS. The Signal Scaling block again down scales the voltage to the range of ± 10 volt, which are the upper and lower limits of digital to analogue converter (GTAO card) of RTDS. The details of conversion is elaborated in the next section. The output signals of the controller, which are the decision commands for interruption of different load feeders (F1-F4) are feed back to the RTDS via analogue to digital converter (GTAO card).

The input and output signals of the controller (the three phase sinusoidal waveforms) are analogue and may be subjected to the noise interference. Two times down scaling of input voltage signals significantly reduces the signal to noise ratio. Although, the output signals are also analogue, since they carry logic levels (0 ≡ 0v ≡ connected and 1 ≡ 5v ≡ disconnected), the noise may not change the voltage levels and therefore, the logic level is more robust against the noise impact comparing to the input signals. The feeder commands are amplified to be applied to the relay and hence, the Circuit Breakers (CBs) in RSCAD is used to apply this ability to power system.

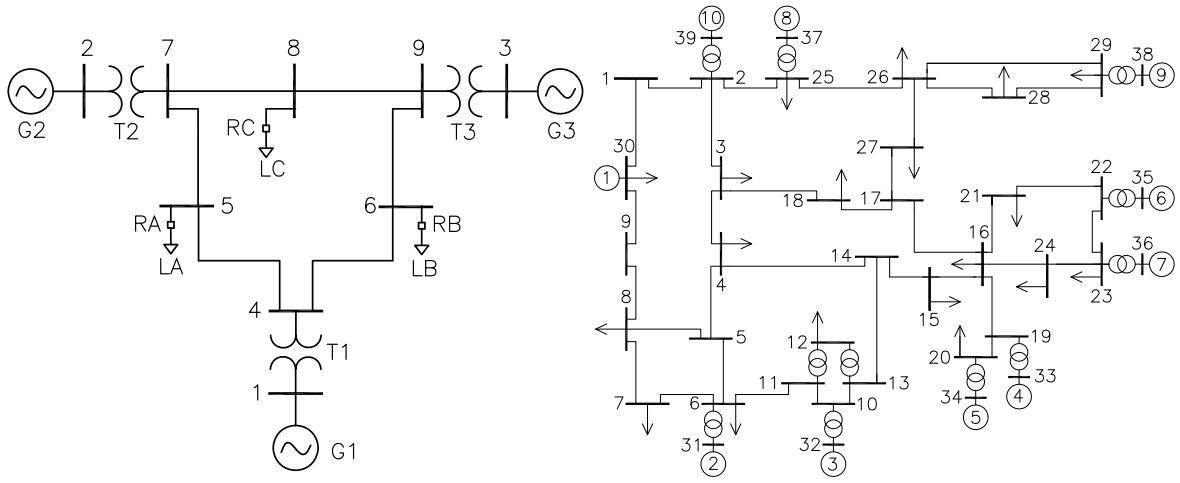

(a) 9 bus IEEE standard test system

(b) 39 bus IEEE standard test system

Figure 8: Scenario 1: G3 outage; measurement accuracy of RTDS and controller at bus 5

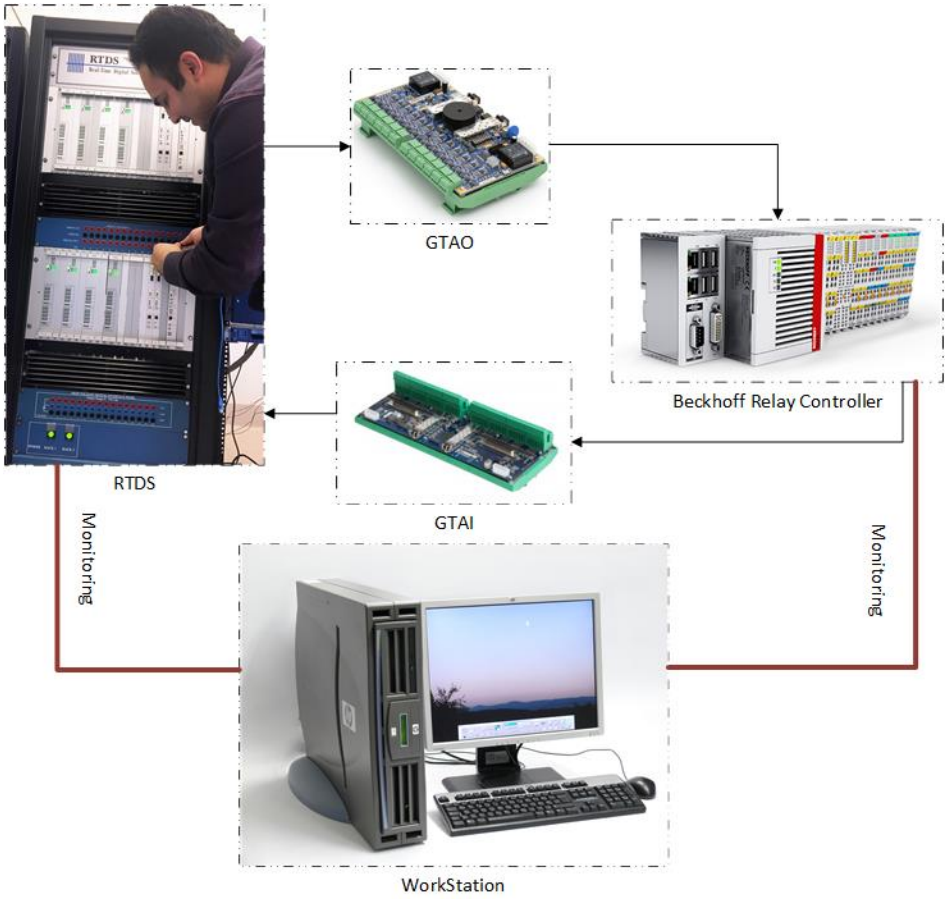

Figure 9: Overall structure of HIL setup

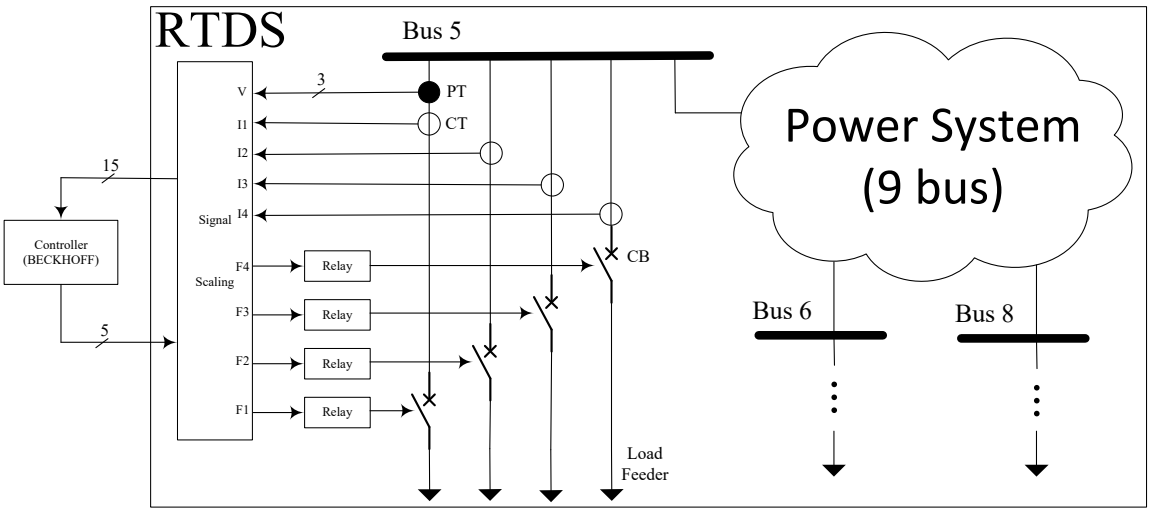

Figure 10: Details of Controller and RTDS interface for load bus 5

5.2 Analogue Signal Scaling & Conversion: RTDS to Controller

The objective of this section is to precisely transfer the measured and commands variables as much as possible from RTDS to the controller and back. The maximum possible of line to line rms voltage ($V_{LLrms}^{\max}$) during abnormal conditions is determined as a surplus percent (x) of nominal voltage V_{LLrms}^{nom} as below:

$$V_{LLrms}^{\max} = (1 + x\%) \cdot V_{LLrms}^{nom} \tag{12}$$

Typical values for x can be found in the manual of protection relays. In order to maximize the accuracy of signal transmission, the variation range of variables corresponding to the aforementioned maximum value should not cross the upper limit of RTDS output voltage equal to +10 volts:

$$\frac{V_{LLrms}^{\max}}{\sqrt{3}} \cdot \sqrt{2} \cdot \frac{5}{S^{RTDS}} = V_{PHamp}^{RTDS} \leq +10 \tag{13}$$

where V_{PHamp}^{RTDS} represents the amplitude of the phase to ground voltage waveform of RTDS. S^{RTDS} stands for down scaling factor of RTDS, in which is calculated based on the following inequality and applied as setting to the GTAO card of RTDS:

$$S_{RTDS} \geq \frac{V_{LLrms}^{\max}}{\sqrt{6}} \tag{14}$$

The down scaled and transmitted values can be converted back to its real and per unit values of line to line rms voltage to be used in the controller algorithm based on equations 15 and 16, respectively:

$$V_{LLrms}^{Cont} = V_{PHamp}^{RTDS} \cdot \frac{S^{RTDS}}{5} \frac{\sqrt{3}}{\sqrt{2}} \tag{15}$$

$$V_{LLrmspu}^{Cont} = \frac{V_{LLrms}^{Cont}}{V_{LLrms}^{nom}} \tag{16}$$

if the phase to ground values are considered in the controller algorithm, the following conversion equations can be instead used:

$$V_{PHrms}^{Cont} = V_{PHamp}^{RTDS} \cdot \frac{S^{RTDS}}{5} \frac{1}{\sqrt{2}} \tag{17}$$

$$V_{PHrmspu}^{Cont} = \frac{V_{PHrms}^{Cont}}{V_{PHrms}^{nom}} \tag{18}$$

5.3 Digital Signal Scaling & Conversion: Controller to RTDS

This section discusses the conversion of controller decision commands from their output voltages to their logical values to be imported to the RTDS. In real application, the controller output is applied to the relay and consequently the relay output as an amplified command is applied to the circuit breaker. Therefore, this conversion is required, if the power system is simulated in RTDS.

This conversion differs from the conversion of sinusoidal waveforms presented in the previous section, due to asymmetrical signal range (0-5v), i.e having offset value. The controller yields $V_{Cont}^{\min}$=0v and $V_{Cont}^{\max}$=5v for 0 and 1 logical levels, respectively. This voltage levels are

converted according to the *conversion*1 mentioned in the equation 19 to fully span and fit the RTDS output range limits:

$$\left\{ \begin{array}{l} V_{Cont}^{\max} = +5 \\ V_{Cont}^{\min} = +0 \end{array} \right\} \xrightarrow{Conversion1} \left\{ \begin{array}{l} V_{RTDS}^{\max} = +10 \\ V_{RTDS}^{\min} = -10 \end{array} \right\} \xrightarrow{Conversion2} \left\{ \begin{array}{l} V_{Cont}^{\max} = +5 \\ V_{Cont}^{\min} = +0 \end{array} \right\} \tag{19}$$

The input signal to the RTDS (V_{RTDS}) can be calculated from controller output voltage (V_{Cont}) as below:

$$V_{RTDS} = S_{RTDS} \cdot (V_{Cont} - V_{Cont}^{offset}) \tag{20}$$

where S_{RTDS} and V_{Cont}^{offset} are scaling factor of RTDS and offset voltage of input signal, respectively:

$$S_{RTDS} = \frac{1}{4} \cdot (V_{Cont}^{\max} - V_{Cont}^{\min}) \tag{21}$$

$$V_{Cont}^{offset} = (V_{Cont}^{\max} - V_{Cont}^{\min})/2 \tag{22}$$

6 Simulation & Experimental Results: (9 Bus) closed loop

6.1 (Controller + Power System) in DIgSILENT PowerFactory

Fig.11 shows the simulation results of G3 outage in DIgSILENT PowerFactory throughout 15 seconds of simulation. Before the contingency at 0.5s, the power system is in the steady state and all of the variables are in the range such as the frequency which is equal to 60 Hz. Following the G3 trip at 0.5s, bus voltages fall almost instantly (fig.11b), whereas frequency is still in the normal range in fig.11a. The variation of voltage is always much larger and faster than the frequency changes [15]. Three load shedding stages (feeders) are triggered same as the RTDS results presented in the previous section. The steady state voltages are almost same, while the frequency is settled at a value, which is lower, but still in range comparing to the RTDS results. Figs.11c and 11d show the active and reactive power of loads following successive load shedding stages.

6.2 closed loop: (Controller + Power System) in RTDS

6.2.1 Scenario 1: Outage of G2

Fig. 12 shows the performance of relays installed at all load buses A, B and C in steady state, before and after outage of largest system generator G2 with 163 MW generation equal to almost 51% of total load. Fig. 12a shows the frequency (F) and frequency thresholds (F_{th}) of different relays, which are stable before the event. Since, 1 pu voltage magnitude is considered as the base for tunning of frequency thresholds instead of different pre-disturbance voltage values, the frequency thresholds in steady state may not be the same as can be seen in fig. 12a.

Following the G2 outage, the frequency starts to suddenly fall and accordingly the frequency thresholds are increased, but with different rate due to difference in voltage drops in load buses (the threshold calculated based on the voltage drop). The loads closer to the event location, experience more voltage drop and hence higher frequency thresholds. After any feeder disconnection, if the voltage profile at corresponding bus is improved comparing to the other buses, the frequency threshold is decreased and therefore, load shedding is fulfilled

at another location. Otherwise, if the voltage profile is still the worse throughout the network, the load shedding is continued at that location. This phenomenon is clearly observable in fig. 12a, since different frequency threshold profiles (F_{th}) are consequently reaching the frequency profiles (F), and therefore, the corresponding feeder is interrupted.

Average frequency value is monitored for activation of load shedding scheme, which means that the load shedding scheme in each relay is triggered if the frequency crosses down F_h=59.5 Hz. Deactivation of scheme in time is necessary to avoid over load shedding. The idea to interrupt as few as possible of the loads can be realized using detection of in-time recovery of frequency above the minimum permissible value. If the recovery of frequency using average frequency trend is distinguished to reach a value above F_h=59.5 Hz in available time period determined by FERC standard, load shedding is stopped [22].

Fig. 12b indicated the voltage profile at load buses. Comparing fig. 12a and fig. 12b reveals that voltage dynamics are much faster than frequency during both outage event and recovery. Frequency and voltage dynamics possess different origin of mechanical and electrical nature,

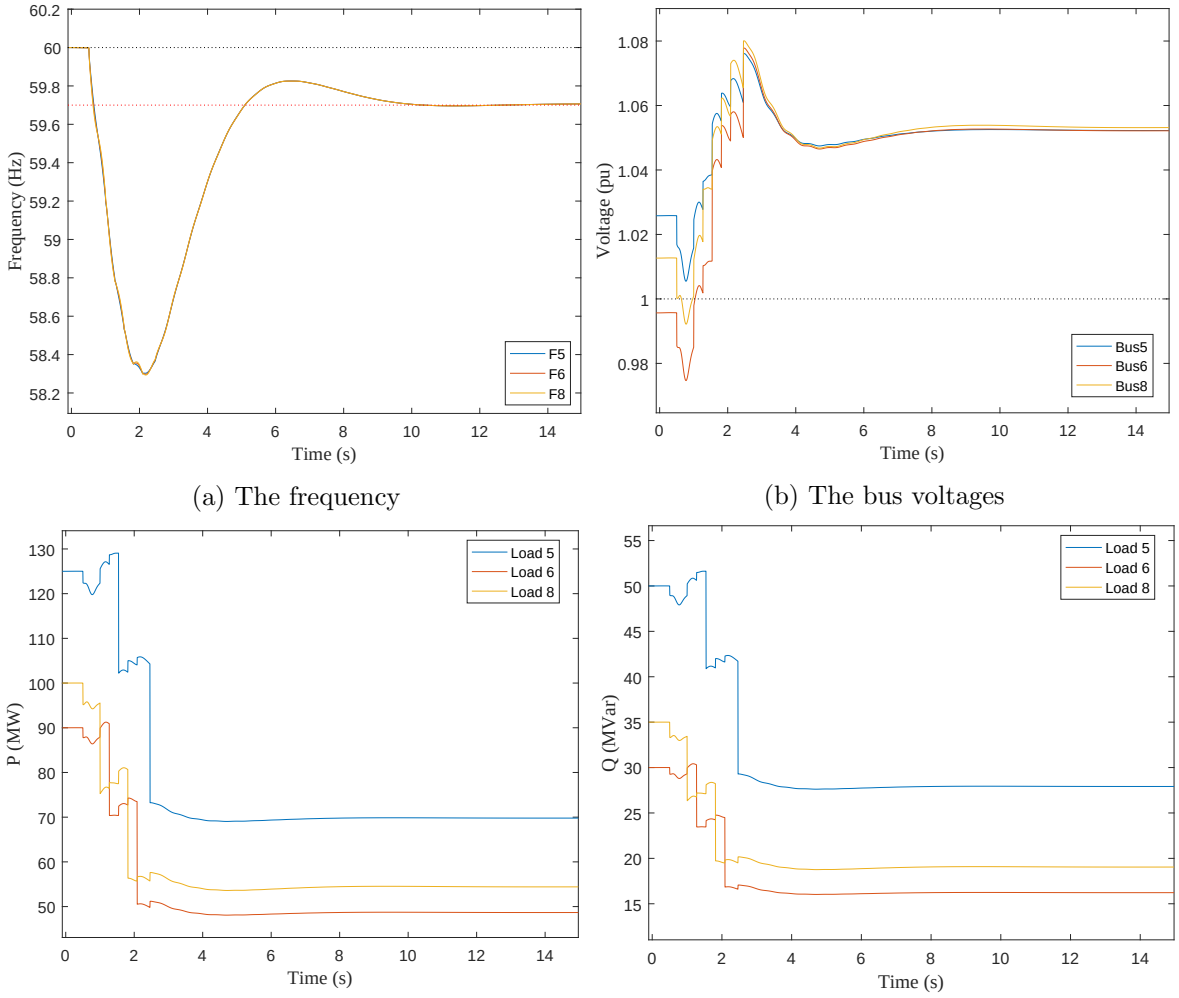

(a) The frequency

(b) The bus voltages

(c) The active power of loads

(d) The reactive power of loads

Figure 11: Load shedding details following outage of G3 in DIgSILENT PowerFactory

respectively.

Figs. 12c and 12d represent active power and number of disconnected feeders in different loads, respectively. Prior to the event, full power demand of feeders are supplied by power system and therefore, there is no interrupted feeder. Following the outage event, the first stage of load 5 (the blue line in fig. 12d) is triggered and hence, its corresponding active power is suddenly reduced in fig. 12c. Consequently, the voltage profiles are slightly improved to a value above 1 pu (fig. 12b). Although, all voltages lie inside the normal range, the amount of interrupted load is not enough to stabilize both frequency and voltage. In this case, the power system suffers form frequency stability rather than voltage stability. Since, the frequency is still out of range and keeps on continuously falling, the load shedding is remained activated.

The second load shedding trial is fulfilled by disconnection of first feeder at load 8, which suppresses the load-generation imbalance, consequently decreases the rate of frequency decline and at the same time increases the bus voltages. The merit of proposed method is in selection of next load shedding location. Instead of curtailing the load in bus 6, it is again done in

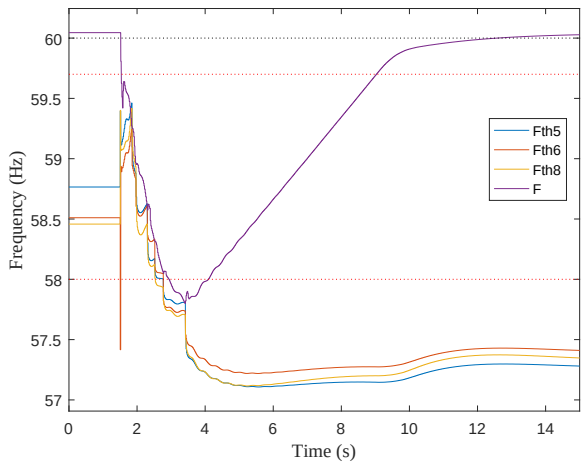

(a) Frequency & relay frequency thresholds

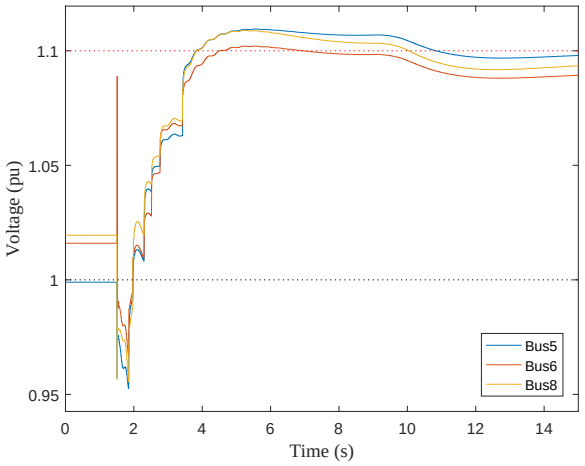

(b) Bus voltages

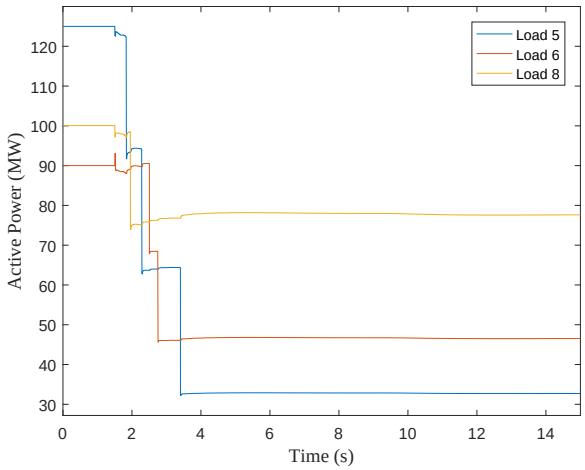

(c) Active power of Loads

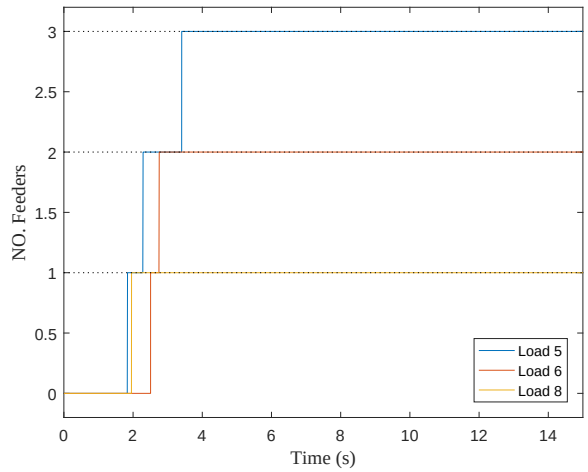

(d) NO of disconnected feeders in each Load bus

Figure 12: Load shedding details following outage of G2 in RTDS

bus 5, due to having lower level of voltage, which is the result of being closer to the event location. To conclude, instead of uniformly distributing the load shedding among available loads, the scheme is concentrates on vicinity of contingency location, which also leads to a reduced amount of shedded load.

Finally, the power system returns to safe and reliable steady state with frequency settlement in a value close to its nominal value, bus voltages below the upper limit. In total, three, one and two feeders of loads are disconnected.

6.2.2 Scenario 2: Outage of G3

Fig. 13 represents the simulation results of outage of G3 generator with capacity of 85 MW equal to 26% of available generation. The generation lost is less comparing to the previous scenario, and thus less load shedding is expected. Fig. 13d shows that only two and one stage of loads 5 and 8 are shed in total, respectively. The adaptive property of proposed method is due to tracking the recovery trend of frequency and shedding as low as possible of load to

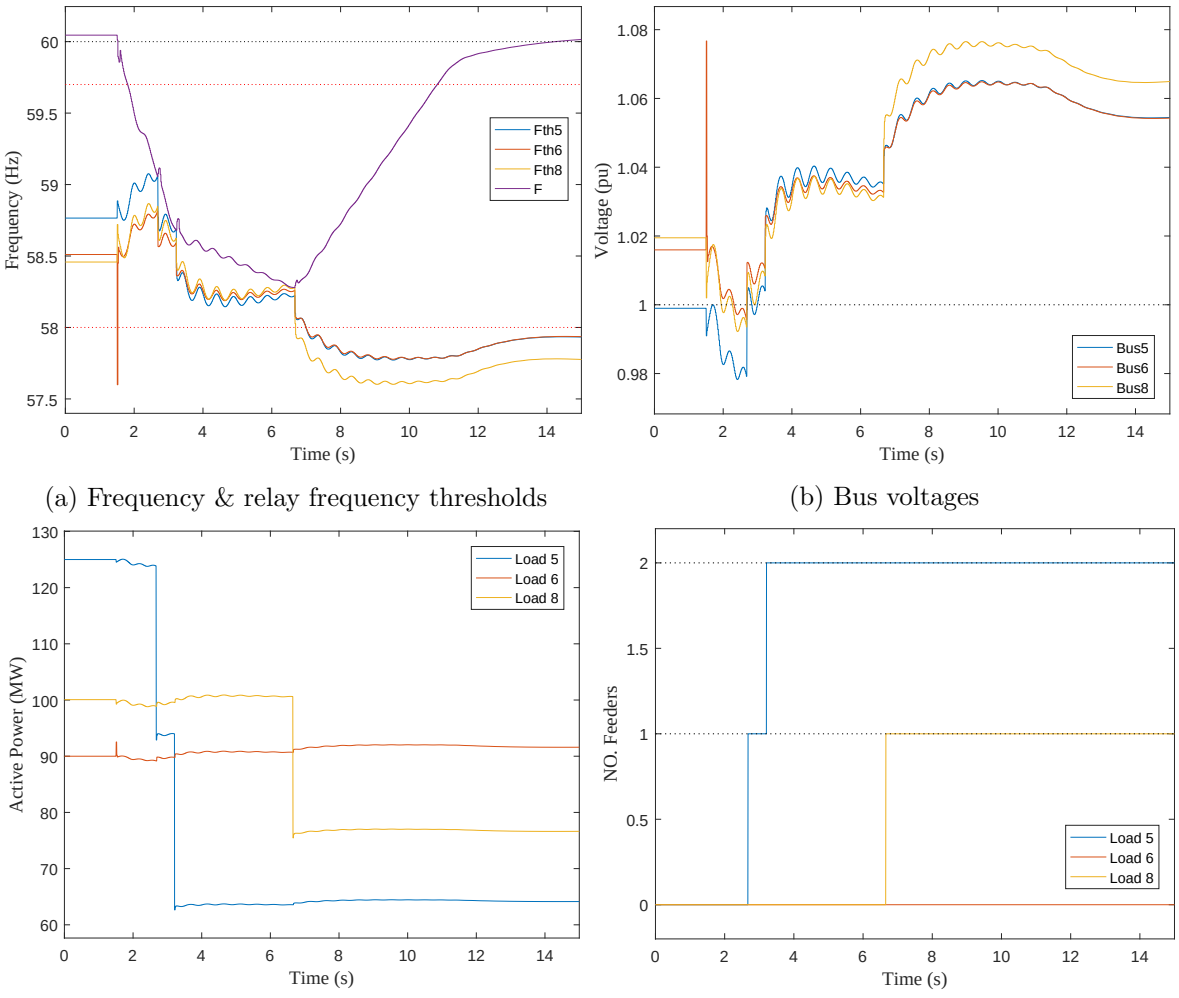

(a) Frequency & relay frequency thresholds

(b) Bus voltages

(c) Active power of Loads

(d) NO of disconnected feeders in each Load bus

Figure 13: Load shedding details following outage of G3 in RTDS

bring the frequency back to the safe region inside its permissible boundary.

Fig. 13a reveals considerable change in slope of frequency drop with major inter area and/or local mode oscillations between seconds 3.3 to 6.5. In this case, the Rate of Change of Frequency (ROCOF) is misleading, unless the average trend of frequency is detected and considered. After the last stage of load shedding, these oscillation are gradually damped and frequency is stabilized around nominal frequency equal to 60 Hz.

Fig. 13b shows the voltage profile at different buses. Although, the voltages are stabilized in range by proper load shedding following the event, the existing oscillatory behavior of frequency profile also appears in the voltage profile and hence in the frequency thresholds, which may affect the decision making of load shedding. Therefore, it is necessary to supervise the frequency derivative variable and track the average trend of frequency and voltage profiles.

According to Figs. 13a and 13d, sharp frequency plunges result in faster crossing of consecutive frequency thresholds by frequency and therefore, less time gap between successive load shedding stages. In contrast, slow or no frequency drop corresponding to small or zero value of ROCOF may cause frequency stuck between two consecutive stages. In this case, the frequency may not trigger more stages and may remain out of range for a long time out of tolerable time of corresponding protection devices.

If the above frequency/voltage-based threshold tunning approach fails in frequency recovery in time, the time/voltage-based backup scheme is automatically activated. The scheme has been illustrated and developed in details in the previous publications of project.

7 Simulation & Experimental Results: (39 Bus) closed loop

7.1 closed loop: Controller + Power System in RTDS

7.1.1 Scenario 1: G2 Outage

The simulation results reflects the performance of relay implemented in RTDS using standard its built-in blocks. Figure. 14 presents the performance of controller as load shedding relay installed at load buses 8, 20 and 29 following outage of G2. Stabilization of power system frequency inside permissible boundary as the main objective of load shedding relay is satisfactorily accomplished. The solid black, red and blue lines in figure. 14a show the frequency thresholds in different load buses. The green line shows the frequency of power system. Note that the "real" in all figures represent measurements from inside controller of RTDS and "measurement" means the measurement from physical controller.

Following the G2 outage, the frequency starts to suddenly fall and accordingly the frequency thresholds are increased, but with different rate due to difference in voltage drops in distinct load buses. The loads closer to the event location, experience more voltage drop and hence higher frequency thresholds. After any feeder disconnection, if the voltage profile at corresponding bus is improved comparing to the other buses, the frequency threshold is decreased and therefore, load shedding is fulfilled at another location. Otherwise, if the voltage profile is still the worse throughout the network, the load shedding is continued at that location. This phenomenon is clearly observable in fig. 14a,

Fig. 14b shows the voltage profile at different buses. Although, the voltages are stabilized in range by proper load shedding following the event, the existing oscillatory behavior of frequency profile also appears in the voltage profile and hence in the frequency thresholds, which may affect the decision making of load shedding. Therefore, it is necessary to supervise

the frequency derivative variable and track the average trend of frequency and voltage profiles.

Figure. 14c represents the ROCOF measurement at each individual load bus. Sharp changes are observable in the profile, which can be suppressed by a utilizing a stronger filter with higher time constant. Increasing the time constant of filter may lead to increase of time latency of ROCOF profile. Therefore, a trade-off and optimize quantity should be chosen to achieve the best performance fo controller.

Figure. 14d shows the number and time of feeder interruption in load buses 8, 20 and 29, which is decided by controller. One feeder of load buses 8 and 20 are successively disconnected and the time gap between successive load shedding is almost 4 seconds. The load shedding is stopped if the frequency recovery trend is recognized to be above the load shedding threshold in time.

The main reason for this problem is partly explained in section 5.2. The RTDS outputs is limited to +- 10V and the controller measuring card designed to being installed in live 3 phase environment with normal voltage transformers (max 410V). This means that we are only using 2,5% of the resolution, and the measurements are therefore more sensitive to noise and signal errors. The same would have been the case on a normal protection!

7.1.2 Scenario 2: G8 Outage

In this scenario, outage of generator G8 is considered as the disturbance for power system. Due to low voltage profile following the first load shedding in load 20, the load shedding is continued in the same load bus. Therefore, in total two stages of load 20 are recognized to be sufficient for frequency recovery. This scenario clearly reflects the advantages of proposed intelligent relay, in which the load shedding location is determined according to the current state of power system instead of already defined location.

Undesired oscillation of voltage profile is directly reflected in the frequency threshold curves. In order to improve the performance of the controller, it can be a good idea to apply a proper filter for obtain smooth and more reliable frequency threshold profiles.

7.2 Online test (closed loop): Power System in RTDS + HIL)

This report, presents the results of decentralized load shedding relays in stabilizing the power system following severe contingencies. In order to evaluate the performance of proposed algorithm, a physical controller is programed with the corresponding C code and connected to the RTDS as Hardware in Loop (HIL). The rest of load shedding relays are simulated inside the RTDS, but their coordination is required to achieve a reliable and efficient emergency control. Same scenarios as previous reports are defined and the performance of controller following each scenario is presented in the next sections.

7.2.1 Scenario 1: G3 Outage

Figure. 16 presents the performance of controller as load shedding relay installed at bus 5 following outage of G3. Stabilization of power system frequency inside permissible boundary as the main objective of load shedding relay is satisfactorily accomplished. The solid blue and red lines in figure. 16a are the result of same calculations using standard blocks available in RTDS and the algorithm implemented in the physical controller out of RTDS, respectively. Comparing the accuracy of frequency measurement in both RTDS and controller reveals that there is some undesired delay between the real values from RTDS and the values measured

by controller), which can be due to calculation of average values to filter out sharp changes in frequency profile.

The behavior of controller in measuring rms voltage indicated in figure. 16b involving of so much sample data in averaging process causes sacrificing fast dynamics of voltage and delay in tracking the trend of voltage variations.

Comparing the frequency curve in figure. 16a with the Rate of Change of Frequency (ROCOF) in 16a shows that inaccurate filtering of measured frequency causes existence of minor oscillations in frequency profile leading to large fluctuations in ROCOF.

Figure. 16d shows the number and time of feeder interruption in load bus 5, which is decided by controller. Two feeders of load bus 5 are successively disconnected and the time gap between successive load shedding is almost 2 seconds. The load shedding is stopped if the frequency recovery trend is recognized to be above the load shedding threshold in time.

Although, the controller task is properly accomplished in this case, the measurement issues may challenge reliability of proposed method. Since precise measurement is easily done in

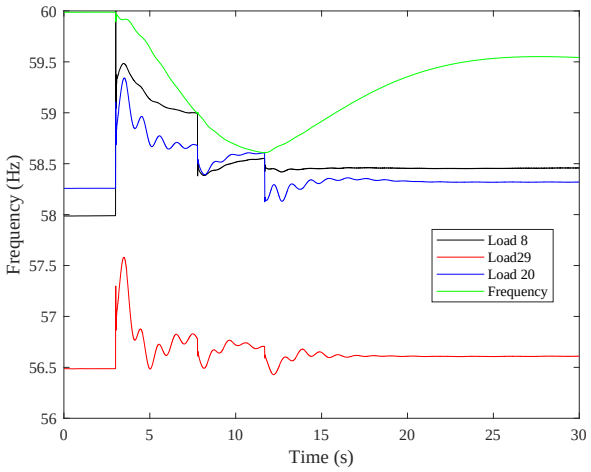

(a) The frequency & frequency thresholds

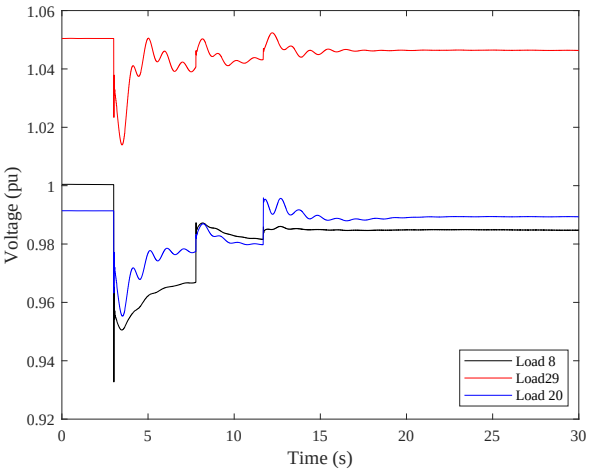

(b) The bus voltages

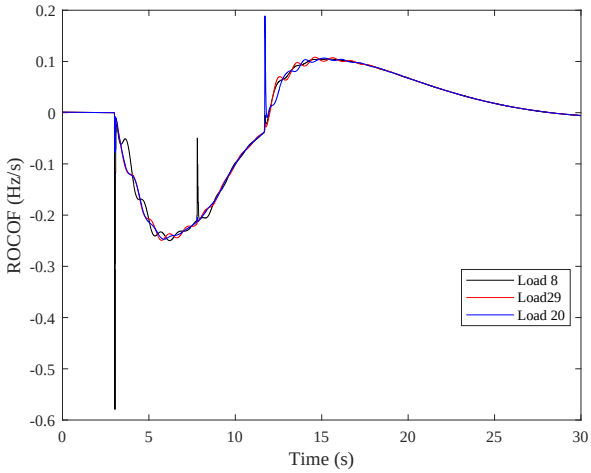

(c) The Rage of Change of Frequency (ROCOF)

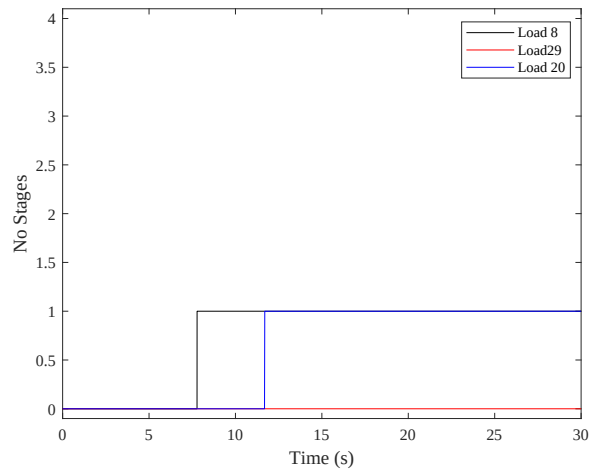

(d) The number of disconnected feeders

Figure 14: Load shedding details following outage of G2: Scenario 1

commercial relays, the issue can be prevailed by improving the measurement algorithm.

7.2.2 Scenario 2: G2 Outage

In this scenario, outage of G2 with the capacity of 51% of available generation is considered as disturbance. Due to severity of contingency, more feeder are interrupted to bring the frequency back to range. Sharp frequency plunge and large negative value of ROCOF in figures. 17a and 17c, respectively, confirms the scale of event. The issues, discussed in the previous section can be observed in the experiment results. Suppressing of undesired fluctuations in the frequency profile is essential. Besides, the filtering of ROCOF dynamics needs to be tunned to detect the real trend of frequency.

Over filtering of voltage profile is obvious in figure. 17b, which leads to tracking the voltage with delay. As a result, speeding up the voltage measurement update rate is among the tasks should be done to improve the performance of relay. Steady state error in voltage profile is

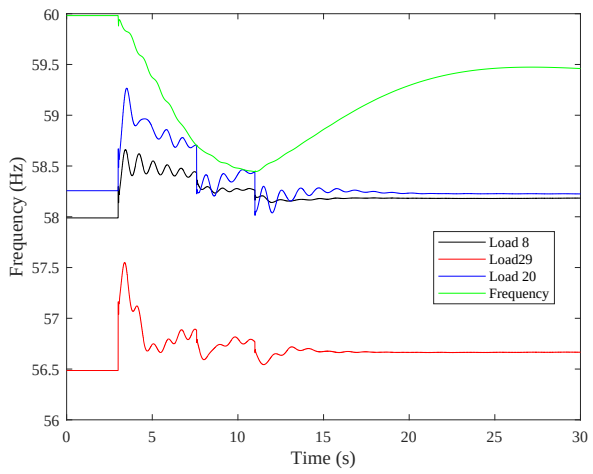

(a) The frequency & frequency thresholds

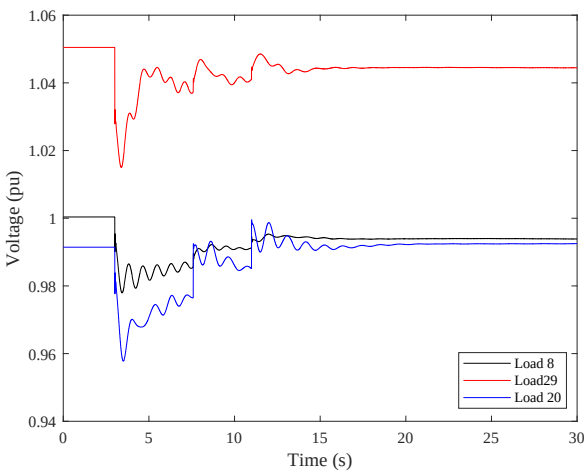

(b) The bus voltages

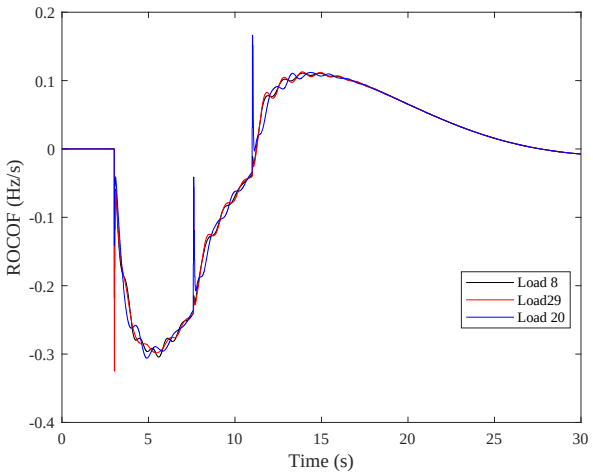

(c) The Rage of Change of Frequency (ROCOF)

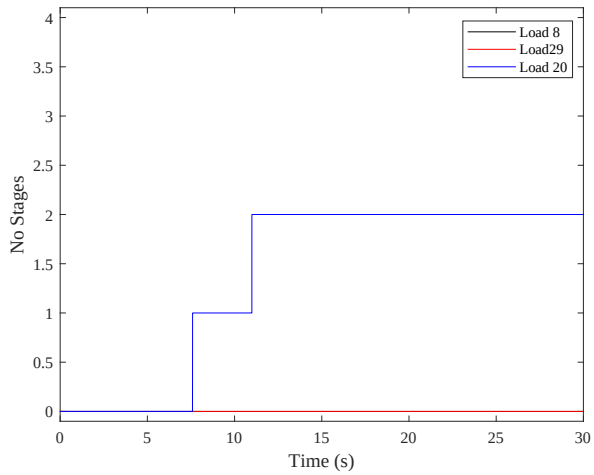

(d) The number of disconnected feeders

Figure 15: Load shedding details following outage of G8: Scenario 2.

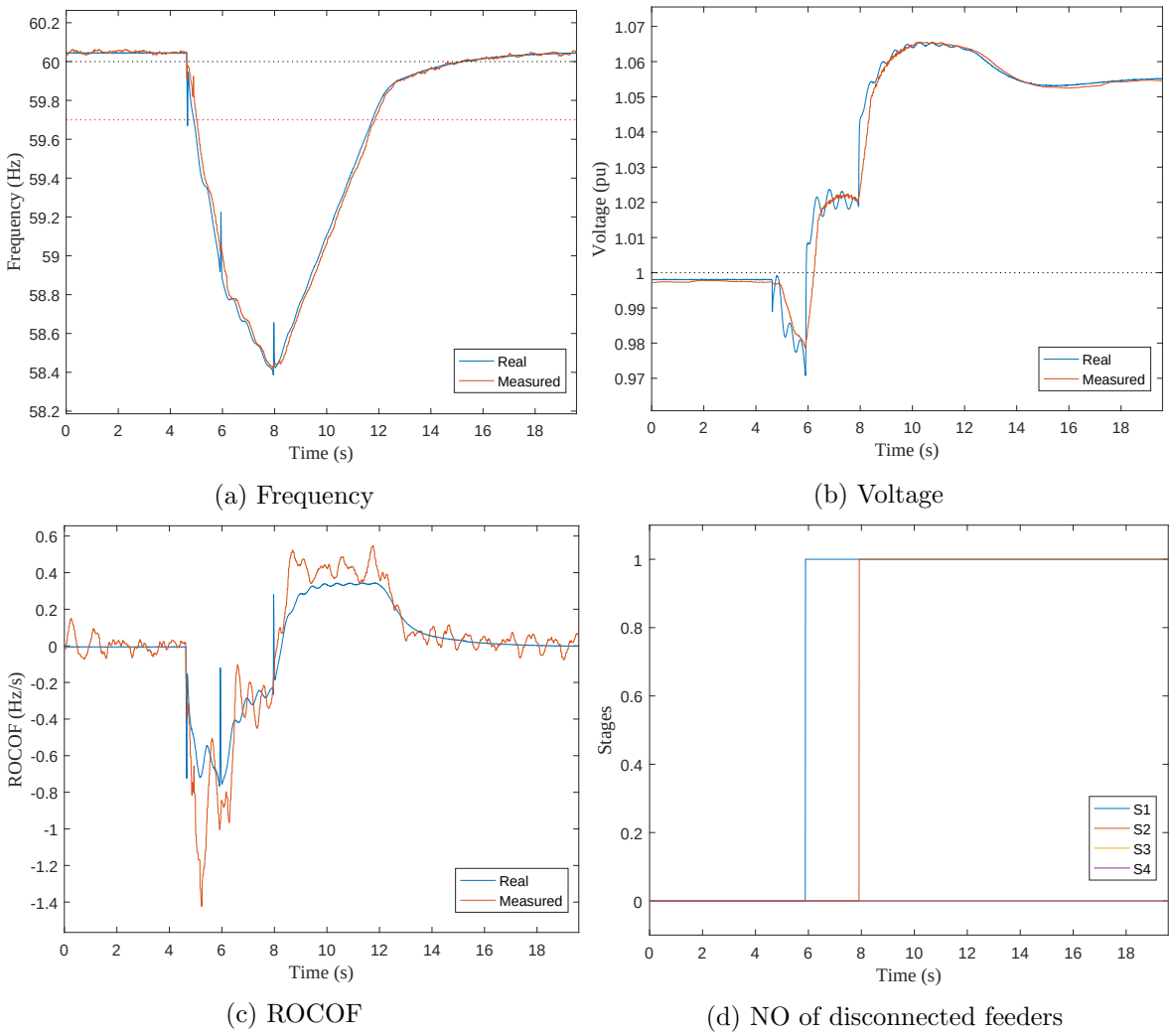

(a) Frequency

(b) Voltage

(c) ROCOF

(d) NO of disconnected feeders

Figure 16: Scenario 1: G3 outage; measurement accuracy of RTDS and controller at bus 5

another issue, which happens due to improper voltage measurement.

8 Field Test (Installation At the Substation)

In this task, the controller is installed at a substation and the controller input signals are provided from substation CTs and PTs connected to the real power system. The main objective of this task is to assess the performance of relay under normal conditions in a real application for a long time to be sure no malfunction operation is occurred by relay. The decision making of relay is monitored and registered. In case of any improper trigger, malfunction or operation failure, required modification and debugging is done to achieve the desired performance.

The controller is installed at the Agersted Substation (Præstbrovej 91, 9330 Dronninglund) based on agreement in coordination meeting with participants of NordEnergy, Inopower, and SALS members at Aalborg University. The controller captured events from the 5th October

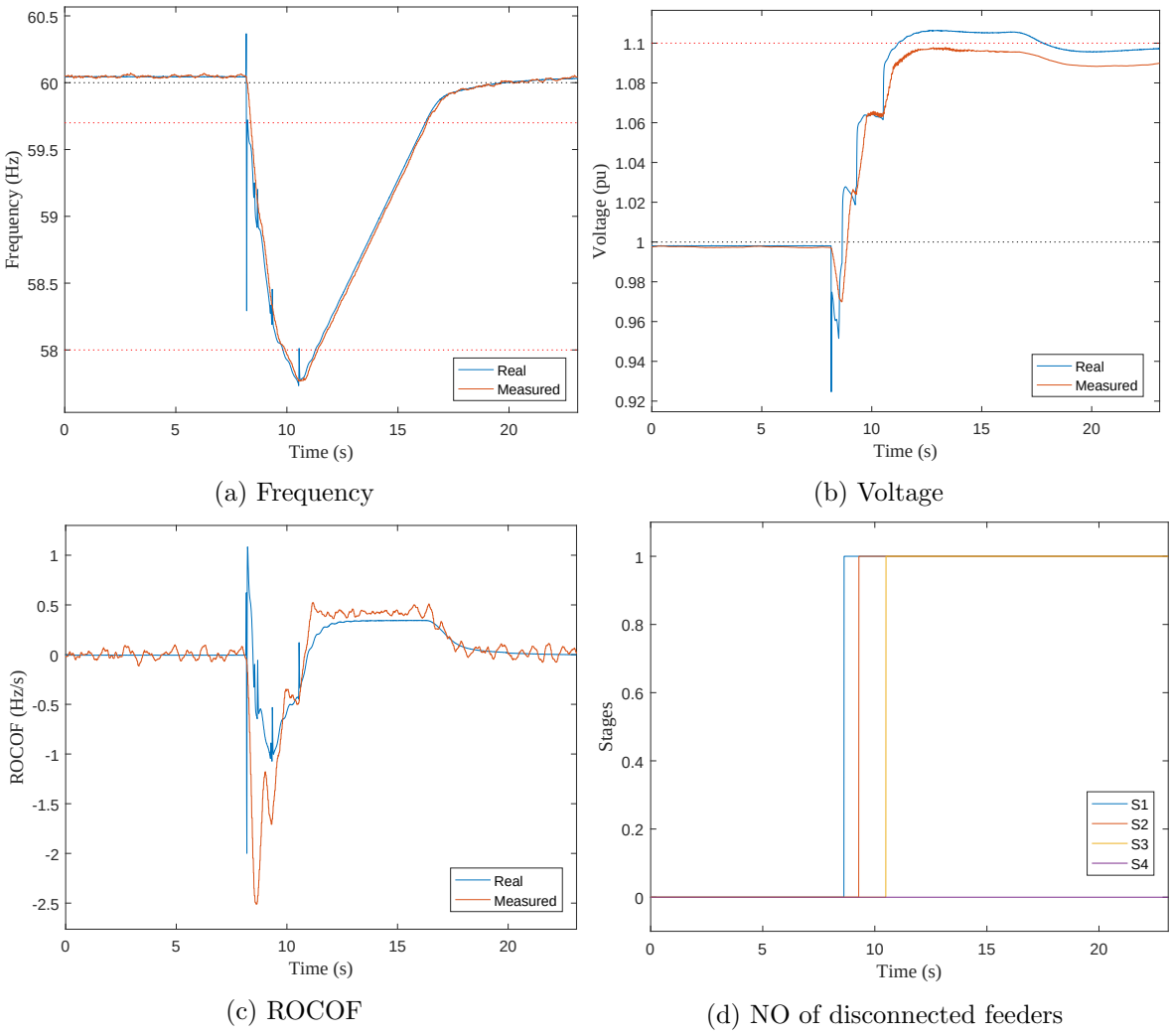

(a) Frequency

(b) Voltage

(c) ROCOF

(d) NO of disconnected feeders

Figure 17: Scenario 2: G2 outage; measurement accuracy of RTDS and controller at bus 5

2018 to the 27th November 2018. The Agersted substation is 60/10 KV class and it was energized by the wind farm on week 38 of 2018. This reason lead to install the controller in the Agersted substation, as mode distortions in the waveforms are expected during the initial operation of the wind turbines the controller triggers are set as follow:

- Voltage value is V and frequency value is f
- $0.94 < V < 1.04\ p.u$
- $50.1 < f < 49.9\ Hz$

The triggers have been acted when values are exist the limit. Therefore, 61 event have been captured based on the triggers act. Summarize of interested results are presented in below.

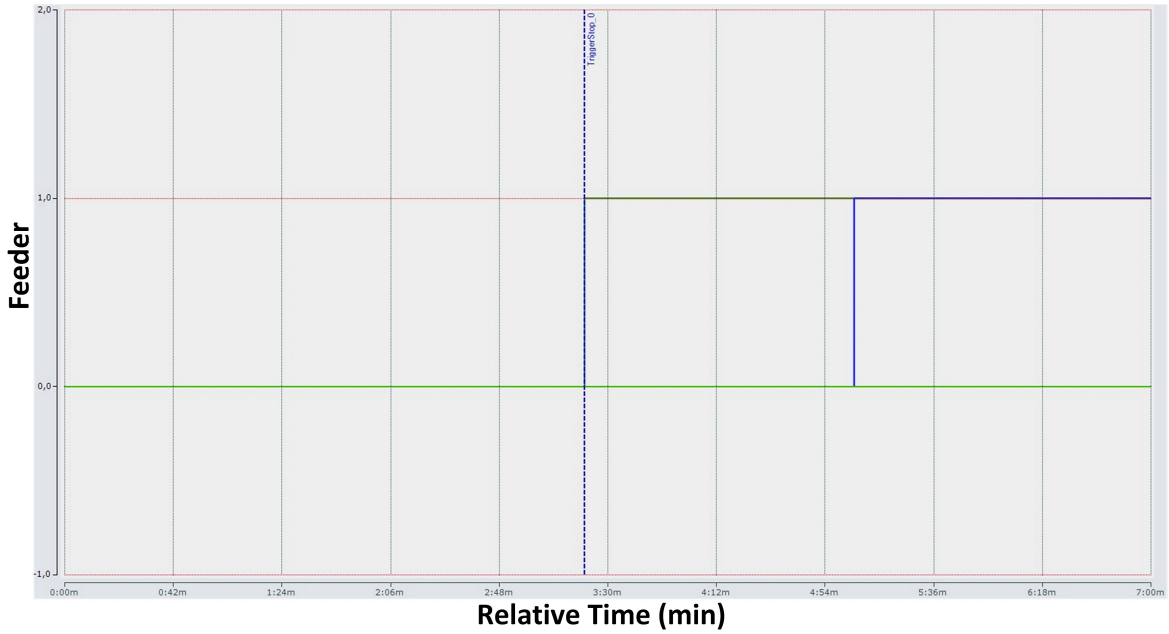

Figure 18: The feeder position in Case study 1 during significant frequency change.

8.1 Case 1

The first event captured on October 22, when the substation energized by connecting wind farm. Fig. 18, 19, 20, and Fig. 21 presents result of this events, which shows the frequency dropping to 0 instantaneously. However by contacting Nordenergy and discussing about this events, its cleared that this event is because of unplugged or lost in power supply of controller, which installed in substation. It is also important to refer that frequency does not drop instantaneously to zero, as seen in the figure and that this situation was not observed again. Fig. 18 presents trigger of feeder 1, which captured from 11:54 AM to 12:51 PM, 22 October. The trigger operated accordingly and attempted to disconnect the load. To avoid this kind of controller trips, a small delay is considered in the algorithm, which means that the estimation from a step forward is also checked and if it was fault in the measurement then controller skip trip. Similarly, the controller will not react to normal faults in the system and wait before procedure with load shedding.

8.2 Case 2

The second case study can be consider as sudden change in voltage magnitude even increase or decrease in this magnitude. The Fig. 22, 23, 24, and Fig. 25 present act of controller during this event. Fig. 22 shows that the voltage changed three times during this event. However. Fig. 25 shows that the controller and algorithm understood the type of change and the trigger was not activated.

8.3 Case 3

The third case study can be consider as sudden change in frequency. The Fig. 26, 27, 28, and Fig. 25 present act of controller during this event. Fig. 26 shows that the frequency

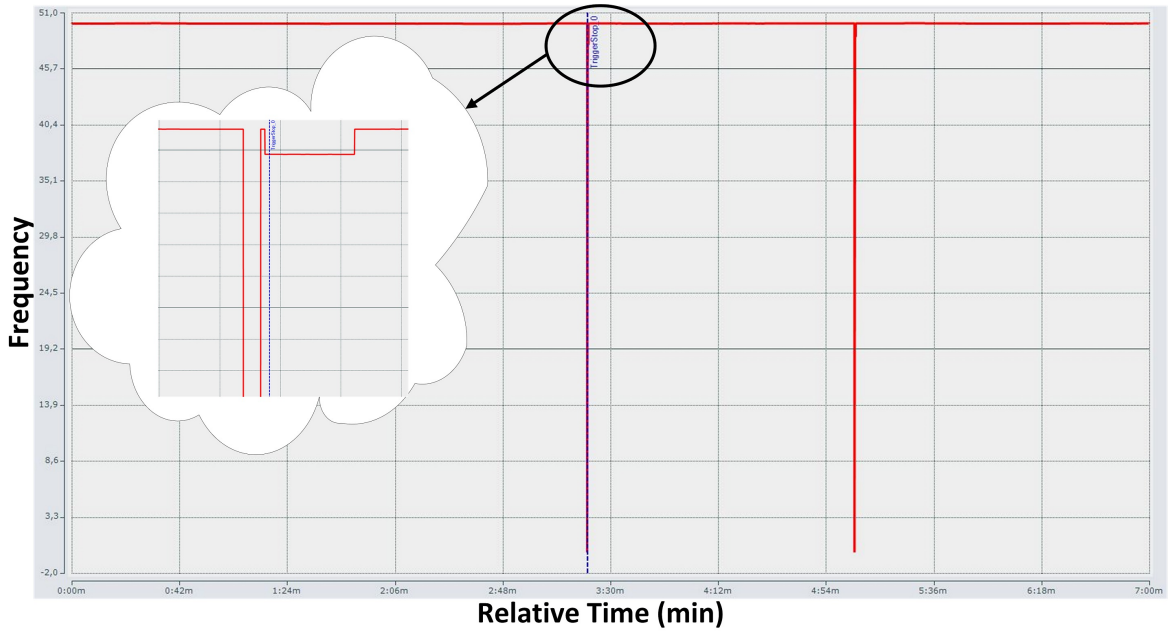

Figure 19: Frequency presentation during Case study 1.

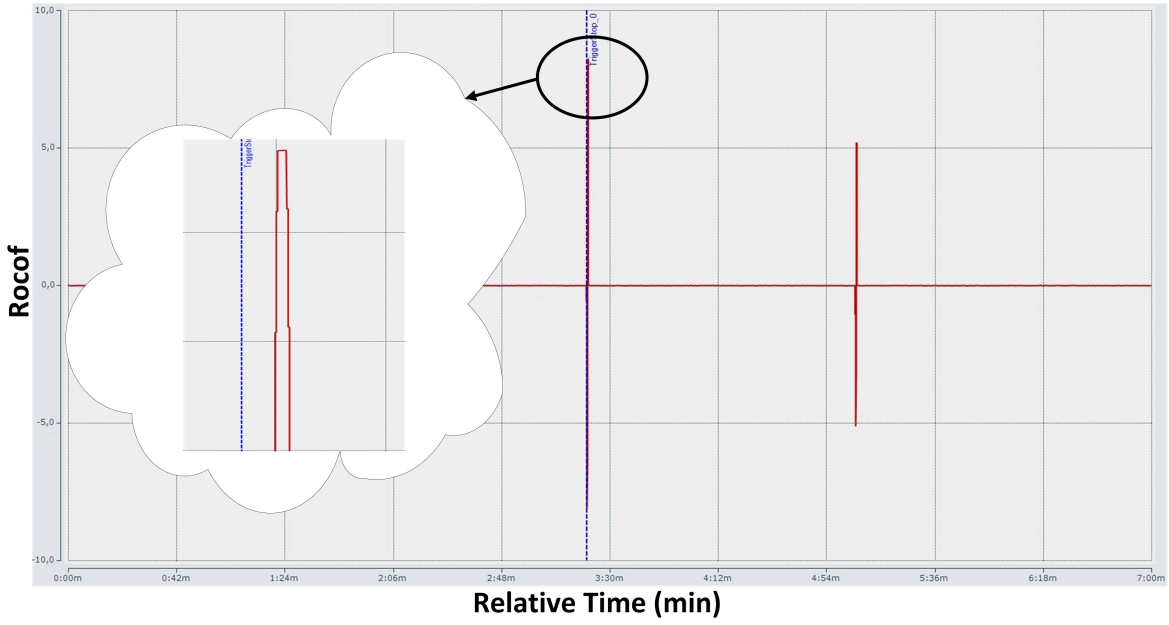

Figure 20: The ROCOF presentation in Case study 1 during significant frequency change.

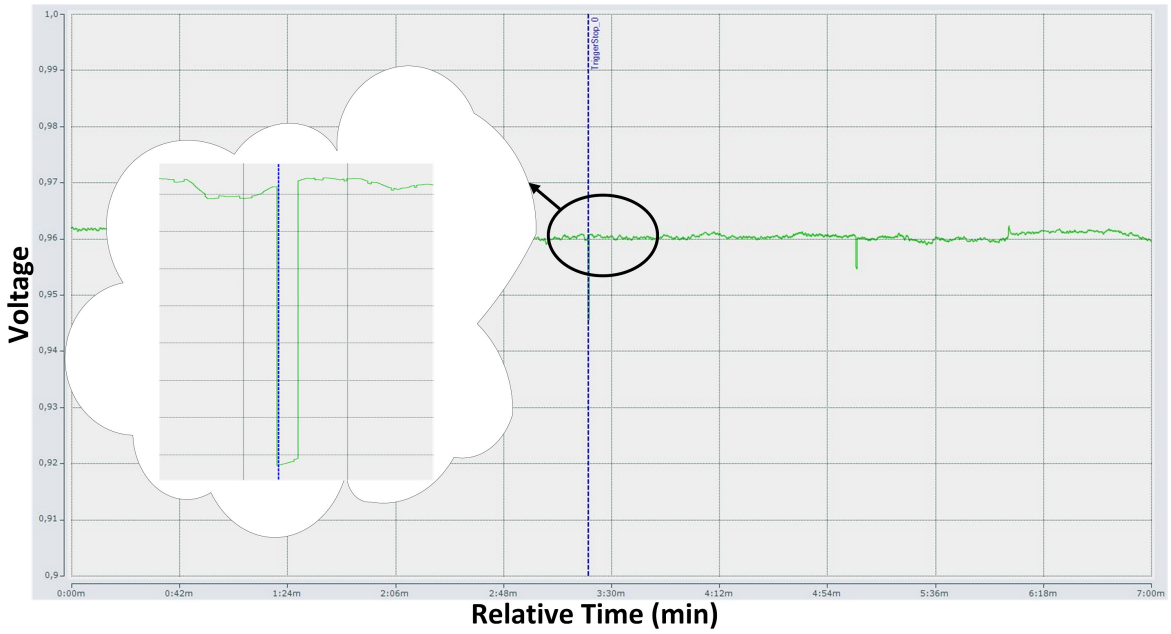

Figure 21: The Voltage presentation in Case study 1 during significant frequency change.

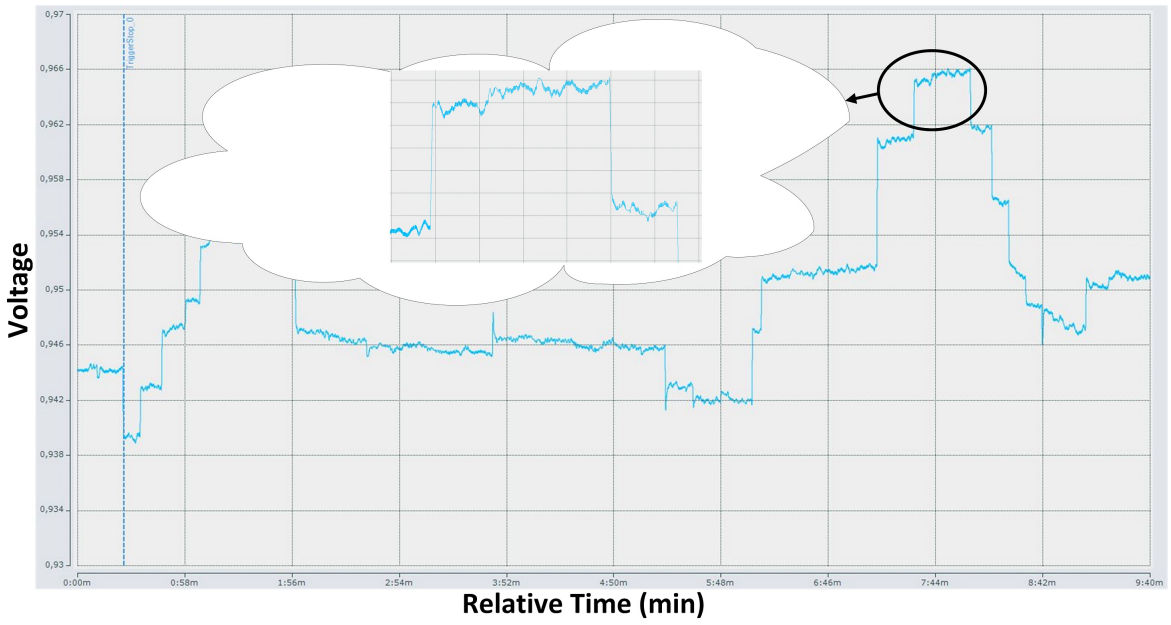

Figure 22: The Voltage presentation in Case study 2 during significant frequency change.

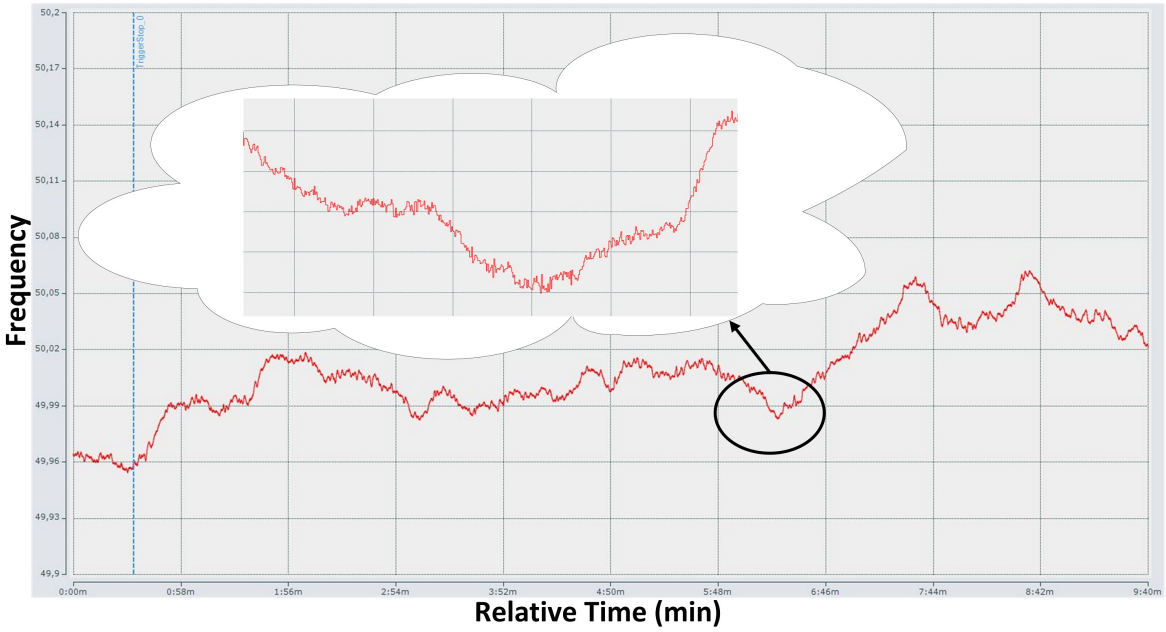

Figure 23: Frequency presentation during Case study 2.

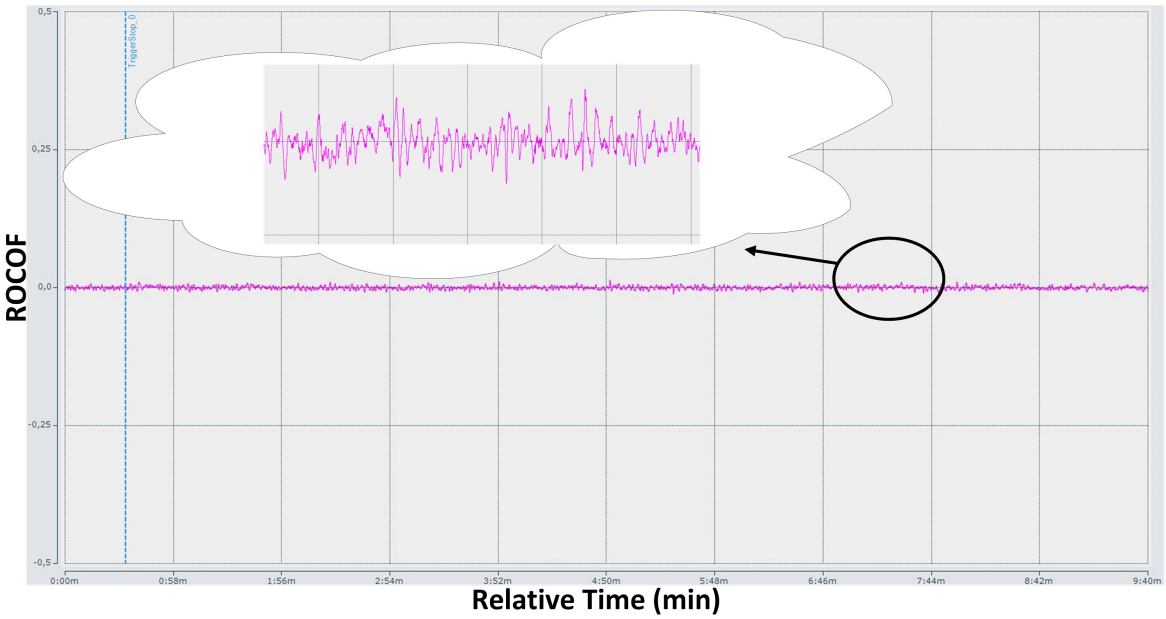

Figure 24: The ROCOF presentation in Case study 2 during significant frequency change.

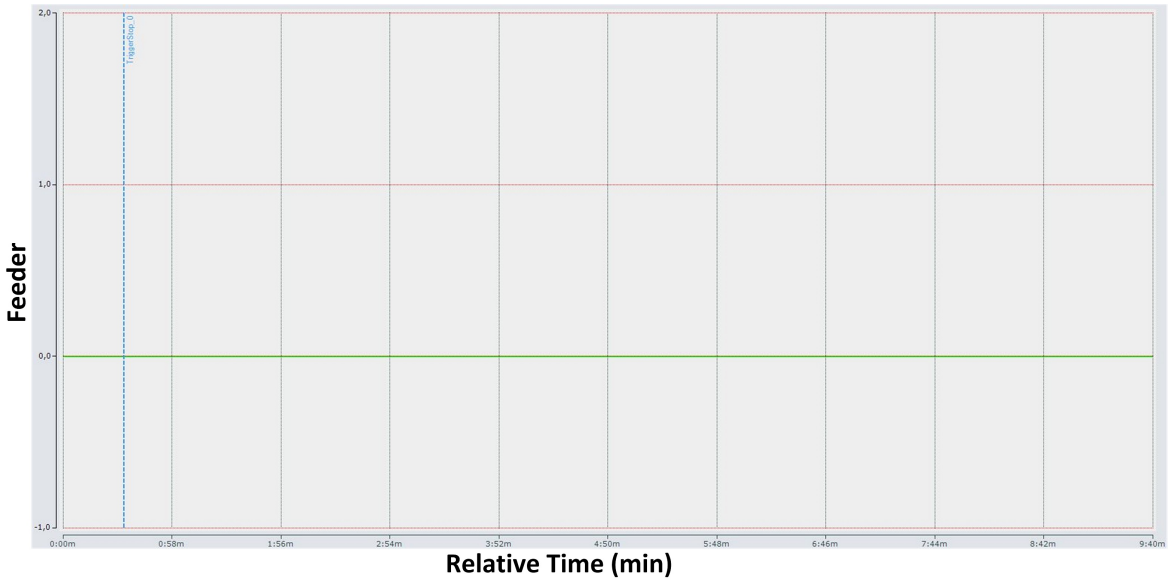

Figure 25: The feeder position in Case study 2 during significant frequency change.

suddenly changed during this event. However. Fig. 29 shows that the controller and algorithm understood the type of change and the trigger was not activated.

9 Conclusion

The project managed to develop an intelligent load-shedding controller, tested as Hardware-In-Loop for different benchmark cases and installed in a 60kV substation for a test period. The controller is able to minimise the amount of load shed during emergency operation, via a decentralised operation not requiring communication and by performing localised load-shedding. This is a big improvement to existing technology, which is not able to adapt load shedding to the specific emergency scenario and thus, does not provide an optimal solution, leading to a disconnection of more consumers than required.

Additionally, the controller considers disperse generation, which is not considered in the existing load-shedding algorithms. This feature is of extra value, as dispersed generation becomes more dominant.

From an implementation perspective, the develop controller is self-contained and it is designed to be used as an add-on with all types of protection relays. Updates can be performed via software updates. All this allows an easier installation and integration with existing power system protection equipment.

10 Future work

Future developments can be made for a more efficient load shedding, as the power system continues evolving. The introduction of battery system at the distribution level, be it directly in dedicated systems or indirectly via electric vehicles, will allow to develop new procedures for load shedding. The principles of the existing controller can still be used, but it will no

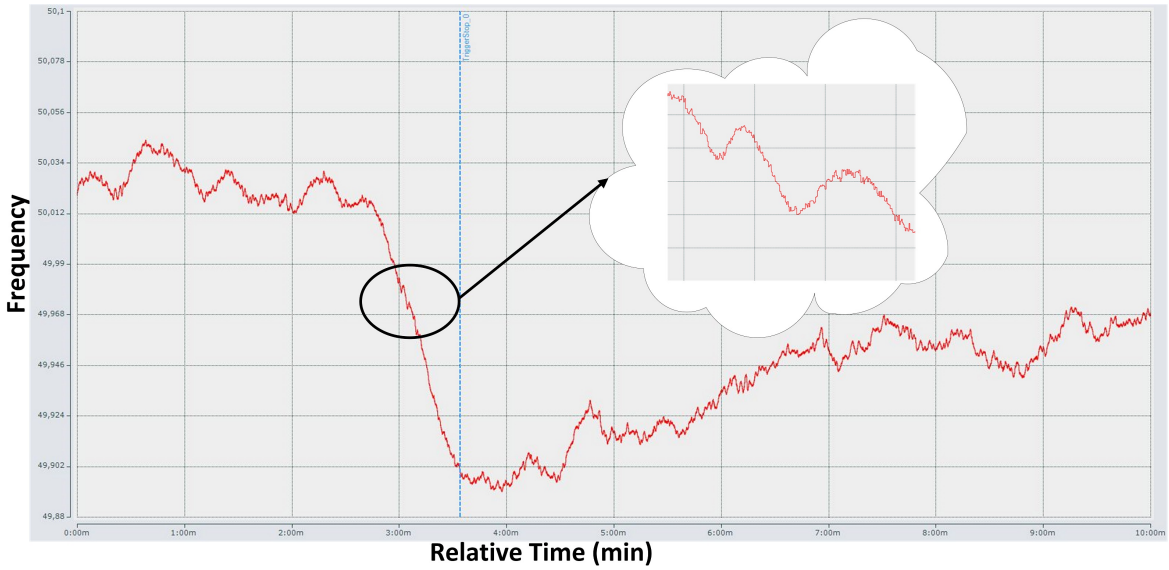

Figure 26: Frequency presentation during Case study 3.

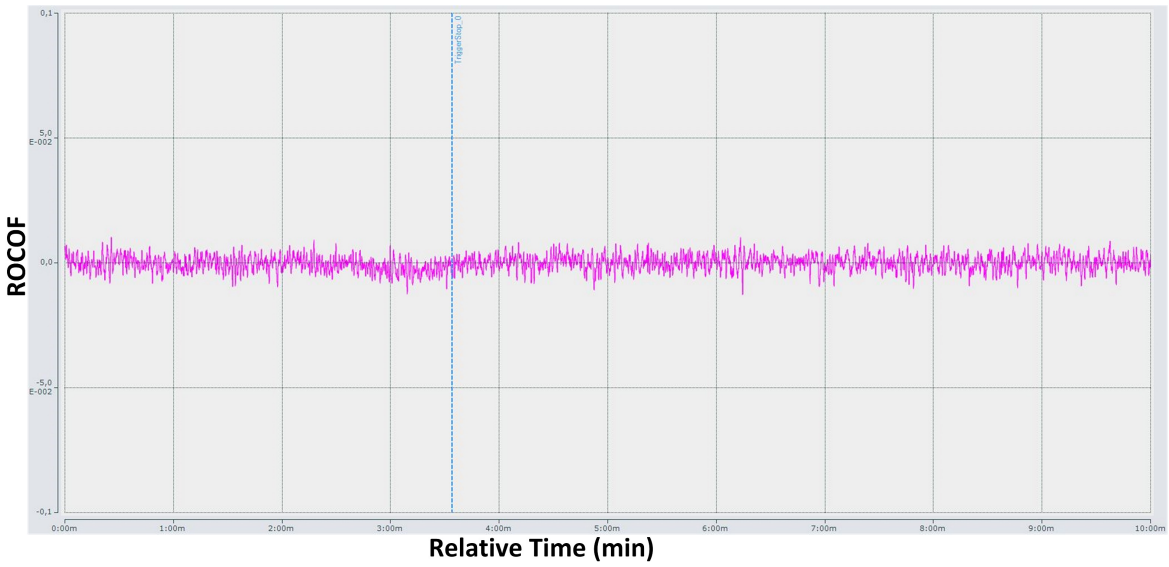

Figure 27: The ROCOF presentation in Case study 3 during significant frequency change.

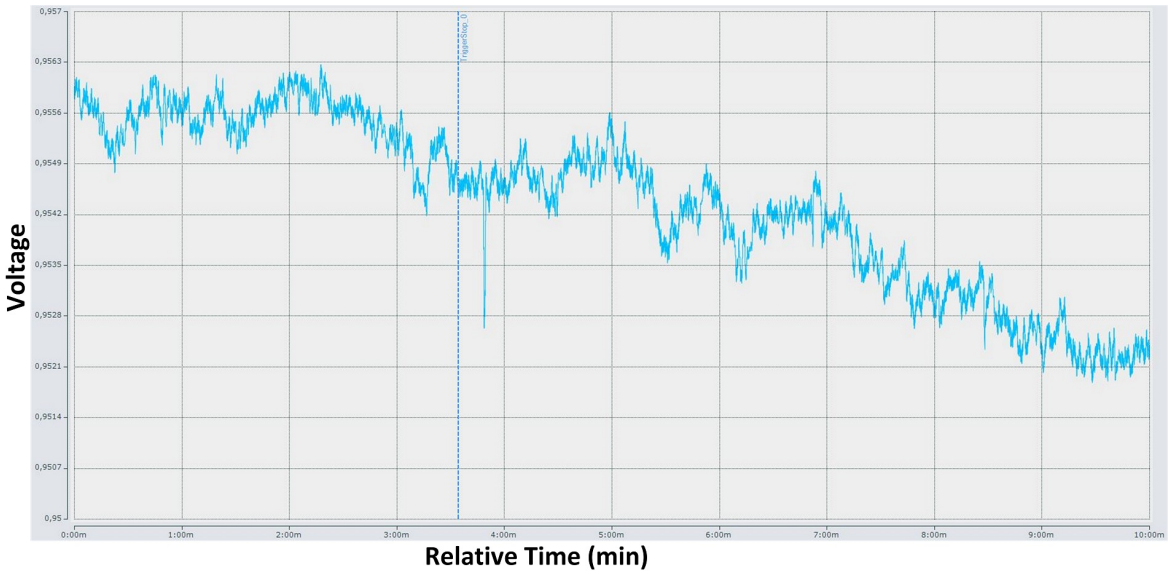

Figure 28: The Voltage presentation in Case study 3 during significant frequency change.

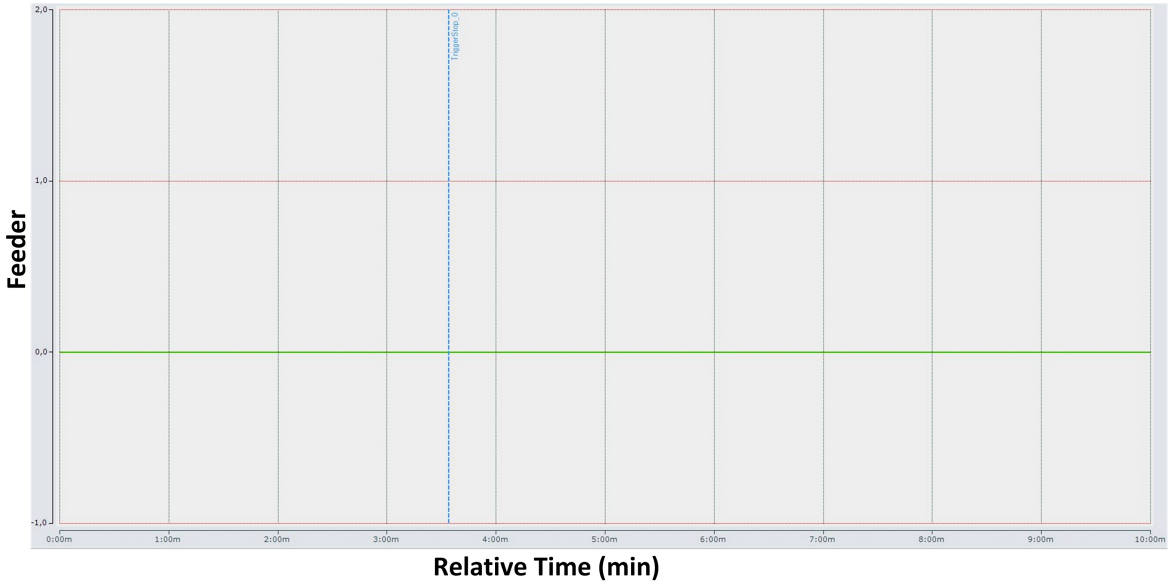

Figure 29: The feeder position in Case study 3 during significant frequency change.

longer provide an optimal reaction and further research/development will be required.

References

[1] H. Bevrani and A. Tikdari, "An ann-based power system emergency control scheme in the presence of high wind power penetration," in *Wind Power Systems*. Springer, 2010, pp. 215–254.

[2] H. Bevrani, T. Hiyama, and A. Tikdari, "On the necessity of considering both voltage and frequency in effective load shedding scheme," in *IEEJ Technical Meeting*, 2009.

[3] U.-C. P. S. O. T. Force, S. Abraham, H. Dhaliwal, R. J. Efford, L. J. Keen, A. McLellan, J. Manley, K. Vollman, N. J. Diaz, T. Ridge *et al.*, *Final Report on the August 14, 2003 Blackout in the United States and Canada: Causes and Recommendations*. US-Canada Power System Outage Task Force, 2004.

[4] G. Andersson, P. Donalek, R. Farmer, N. Hatziargyriou, I. Kamwa, P. Kundur, N. Martins, J. Paserba, P. Pourbeik, J. Sanchez-Gasca *et al.*, "Causes of the 2003 major grid blackouts in north america and europe, and recommended means to improve system dynamic performance," *Power Systems, IEEE Transactions on*, vol. 20, no. 4, pp. 1922–1928, 2005.

[5] Y. Wang, I. Pordanjani, W. Li, W. Xu, and E. Vaahedi, "Strategy to minimise the load shedding amount for voltage collapse prevention," *Generation, Transmission & Distribution, IET*, vol. 5, no. 3, pp. 307–313, 2011.

[6] P. Kundur, *Power system stability and control*. Tata McGraw-Hill Education, 1994.

[7] IEEE, "Ieee guide for the application of protective relays used for abnormal frequency load shedding and restoration," *IEEE Std C37.117-2007, Power System Relaying Committee*, pp. 1–43, 2007.

[8] U. Rudez and R. Mihalic, "Monitoring the first frequency derivative to improve adaptive underfrequency load-shedding schemes," *Power Systems, IEEE Transactions on*, vol. 26, no. 2, pp. 839–846, 2011.

[9] U. Rudez and R. Mihalic, "Analysis of underfrequency load shedding using a frequency gradient," *Power Delivery, IEEE Transactions on*, vol. 26, no. 2, pp. 565–575, 2011.

[10] H. Liu, A. Bose, and V. Venkatasubramanian, "A fast voltage security assessment method using adaptive bounding," *Power Systems, IEEE Transactions on*, vol. 15, no. 3, pp. 1137–1141, 2000.

[11] A. Saffarian and M. Sanaye-Pasand, "Enhancement of power system stability using adaptive combinational load shedding methods," *Power Systems, IEEE Transactions on*, vol. 26, no. 3, pp. 1010–1020, 2011.

[12] M. Q. Ahsan, A. H. Chowdhury, S. S. Ahmed, I. H. Bhuyan, M. A. Haque, and H. Rahman, "Technique to develop auto load shedding and islanding scheme to prevent power system blackout," *Power Systems, IEEE Transactions on*, vol. 27, no. 1, pp. 198–205, 2012.

[13] K. Seethalekshmi, S. Singh, and S. Srivastava, "A synchrophasor assisted frequency and voltage stability based load shedding scheme for self-healing of power system," *Smart Grid, IEEE Transactions on*, vol. 2, no. 2, pp. 221–230, 2011.

[14] IEEE, "Ieee standard definitions for power switchgear," *IEEE Std C37.100-1992*, 1992.

[15] J. Tang, J. Liu, F. Ponci, and A. Monti, "Adaptive load shedding based on combined frequency and voltage stability assessment using synchrophasor measurements," *Power Systems, IEEE Transactions on*, vol. 28, no. 2, pp. 2035–2047, 2013.

[16] H. Bevrani, G. Ledwich, and J. J. Ford, "On the use of df/dt in power system emergency control," in *Power Systems Conference and Exposition, 2009. PSCE'09. IEEE/PES*. IEEE, 2009, pp. 1–6.

[17] B. Hoseinzadeh, F. Faria Silva, and C. Leth Bak, "Power system stability using decentralized under frequency and voltage load shedding," *PES General Meeting Conference Exposition, 2014 IEEE*, pp. 1–5, 2014.

[18] B. Hoseinzadeh, F. Faria Silva, and C. Leth Bak, "Adaptive tuning of frequency thresholds using voltage drop data in decentralized load shedding," *Power Systems, IEEE Transactions on*, vol. 30, no. 4, pp. 2055–2062, July 2015.

[19] Y.-Y. Hong, M.-C. Hsiao, Y.-R. Chang, Y.-D. Lee, and H.-C. Huang, "Multiscenario underfrequency load shedding in a microgrid consisting of intermittent renewables," *Power Delivery, IEEE Transactions on*, vol. 28, no. 3, pp. 1610–1617, 2013.

[20] A. Ghaleh, M. Sanaye-Pasand, and A. Saffarian, "Power system stability enhancement using a new combinational load-shedding algorithm," *Generation, Transmission & Distribution, IET*, vol. 5, no. 5, pp. 551–560, 2011.

[21] H. Seyedi and M. Sanaye-Pasand, "New centralised adaptive load-shedding algorithms to mitigate power system blackouts," *Generation, Transmission & Distribution, IET*, vol. 3, no. 1, pp. 99–114, 2009.

[22] NERC, "Nerc standard on automatic underfrequency load shedding," *Reliability Standards for the Bulk Electric Systems of North America*, pp. 1479–1518, 2017.

[23] P. Kundur, J. Paserba, V. Ajjarapu, G. Andersson, A. Bose, C. Canizares, N. Hatziargyriou, D. Hill, A. Stankovic, C. Taylor *et al.*, "Definition and classification of power system stability ieee/cigre joint task force on stability terms and definitions," *Power Systems, IEEE Transactions on*, vol. 19, no. 3, pp. 1387–1401, 2004.

[24] "Ieee guide for protective relay applications to transmission lines," *IEEE Std C37.113-2015*, pp. 1–141, June 2016.

[25] IEEE, "Ieee guide for ac generator protection," *IEEE Std C37.102, Power System Relaying Committee*, vol. 37, pp. 1–190, 2013.

[26] P. M. Anderson and A. A. Fouad, *Power system control and stability*. John Wiley & Sons, 2008.